LOW SOLAR ABSORPTANCE AND EMITTANCE SURFACES UTILIZING VACUUM DEPOSITED TECHNIQUES

Report No. CR-73039

4-06-66-13 October 1966

Contract No. NAS 2-3063

Final Report for Period
29 June 1965 to 28 September 1966

Prepared for

NASA
Ames Research Center
Moffett Field, California

LOCKHEED PALO ALTO RESEARCH LABORATORY
LOCKHEED MISSILES & SPACE COMPANY
A GROUP DIVISION OF LOCKHEED AIRCRAFT CORPORATION

APPROVED: R. P. Caren

R. P. Caren
Member, Thermophysics
Aerospace Sciences Laboratory

S. A. Greenberg
Member, Thermophysics
Aerospace Sciences Laboratory

D. A. Vance
Member, Thermophysics
Aerospace Sciences Laboratory

FOREWORD

This report was prepared by the Thermophysics Section of the Aerospace Sciences Laboratory, Lockheed Missiles & Space Company for NASA – Ames Research Center, Moffett Field, California, as the final report under contract NAS 2-3063. The work described was performed during the period 29 June 1965 to 28 September 1966.

ABSTRACT

An investigation was made of the techniques and materials for finishing spacecraft structural surfaces with stable, reproducible, thermal control materials. Various coating systems, prepared by vacuum physical vapor deposition, were evaluated in terms of optical characteristics. Basic system parameters were deposition rate, film thickness, substrate material, and finish. Coating systems of interest were those with low solar absorptance (α_s), low infrared emittance (ϵ), and ratios of absorptance to emittance (α_s/ϵ) varying from 2.0 to 0.07. Optical measurements were made of specimens before and after irradiation, with substrates at 294°K and 533°K during irradiation. Results are evaluated in terms of both the morphology of the coating systems and the kinetics due to ultraviolet irradiation and thermal diffusion. Coating systems were selected to satisfy practical engineering requirements. These systems were, (1) quartz substrates with second surface silver for low α_s, (2) polished aluminum alloy substrate with silver overcoated with silica for α_s/ϵ of 1.0 and low α_s, and (3) mill-finish aluminum alloy with silver and alumina overcoat for low ϵ. The systems showed no significant change in absorptance or emittance when subjected to 2000 ESH (equivalent sun-hours) at 294° K. Exposure to 2000 ESH at 533° K resulted in a change in the solar absorptance of one system. This change is ascribed to diffusion and structure change.

SUMMARY

Twenty-four systems were selected for screening tests in a vacuum ultraviolet environment at a substrate temperature of 533°K for 250 sun-hours at a 10-sun intensity. This test also included thermal cycling.

Selections were made of three systems based on the results of the screening tests and practical engineering materials requirements. The three selected systems were then exposed to a 2000 sun-hour vacuum ultraviolet environment with substrates at 294°K and 533°K.

The following systems were selected after optical measurements were made of specimens subjected to the 2000 sun-hour exposure at 533°K:

(1) α_s/ϵ less than 0.1 $\alpha_s = 0.052$, $\epsilon_L = 0.74$

Fused silica with evaporated silver [OSR-TP-060 (Ref. 1)]

(2) $\alpha_s/\epsilon \approx 1.0$, α_s less than 0.1 $\alpha_s = 0.072$, $\epsilon_L = 0.07$

Polished 6061-T6 aluminum alloy with silver and 3000 Å overcoat of silica

(3) Minimum emittance $\alpha_s = 0.074$, $\epsilon_L = 0.03$

Mill-finished 6061-T6 aluminum alloy with silver and 1000 Å overcoat of alumina

ACKNOWLEDGMENTS

The authors gratefully acknowledge the advise, assistance, and continued interest of Mr. E. R. Streed of the NASA-Ames Research Center, who served as technical monitor for this program. Appreciation for their cooperating in performing spectral reflectance and normal emittance measurements is accorded to the Thermophysics Laboratory of TRW, Inc. The efforts of the members of the Thermophysics group of LMSC in support of this program are acknowledged, and particular appreciation is directed to Mr. R. L. Olson for his original conception and development of the Optical Solar Reflector.

CONTENTS

Section		Page
	FOREWORD	iii
	ABSTRACT	iv
	SUMMARY	v
	ACKNOWLEDGMENTS	vi
	ILLUSTRATIONS	ix
	TABLES	xi
	NOMENCLATURE	xii
1	INTRODUCTION	1-1
	1.1 Objective and Approach	1-1
	1.2 Coating Systems	1-1
	1.3 Substrate Requirements	1-2
	1.4 Environmental Stability Studies	1-2
	1.5 Measurements	1-3
2	SAMPLE PREPARATION	2-1
	2.1 Optical Solar Reflector	2-1
	2.2 Deposition Substrates	2-1
3	MATERIAL DESCRIPTION	3-1
	3.1 Vacuum Deposition Source Material	3-1
	3.2 Substrates	3-2
	3.3 OSR-TP-060	3-3
4	EQUIPMENT AND APPARATUS	4-1
	4.1 Electron Beam Vacuum Evaporation System	4-1
	4.2 Optical Measurement Equipment	4-5
	4.3 Environmental Test Equipment	4-13

Section		Page
5	EXPERIMENTAL PROCEDURES	5-1
	5.1 OSR Procedure	5-1
	5.2 Deposited Optical Films	5-1
6	EXPERIMENTAL RESULTS	6-1
	6.1 OSR Adhesive Evaluation	6-1
	6.2 Deposited Coating Systems	6-3
	6.3 Optical Characteristics	6-12
	6.4 Ultraviolet Environmental Test Results and Optical Measurements	6-17
7	DISCUSSION	7-1
	7.1 Vapor-Deposited Films	7-1
	7.2 Optical Measurements	7-3
8	CONCLUSIONS	8-1
9	RECOMMENDATIONS	9-1
10	REFERENCES	10-1

ILLUSTRATIONS

Figure		Page
4-1	Electron Beam Evaporation System	4-2
4-2	Electron Beam Evaporation System Schematic	4-3
4-3	Substrate Holder	4-6
4-4	Upper Support Structure	4-7
4-5	Low-Temperature Emittance Apparatus	4-8
4-6	Schematic of Low-Temperature Emittance Apparatus	4-9
4-7	Blackbody Receiver Calibration Curve	4-11
4-8	Typical Time Required To Attain Radiator and Receiver Temperature Equilibrium	4-12
4-9	Ultraviolet Radiation-High Vacuum Exposure Apparatus	4-14
6-1	Silica-Aluminum-Glass System – Solar Absorptance α_S and Emittance ϵ_L Versus Silica Film Thickness (No Crucible)	6-13
6-2	Silica-Aluminum-Glass System – Solar Absorptance α_S and Emittance ϵ_L Versus Silica Film Thickness (Alumina Crucible)	6-13
6-3	Alumina-Aluminum-Glass System – Solar Absorptance α_S and Emittance ϵ_L Versus Alumina Film Thickness (No Crucible)	6-14
6-4	Alumina-Aluminum-Glass System – Solar Absorptance α_S and Emittance ϵ_L Versus Alumina Film Thickness (Alumina Crucible)	6-14
6-5	Alumina-Gold-Glass System – Solar Absorptance α_S and Emittance ϵ_L Versus Alumina Film Thickness	6-15
6-6	Silica-Silver-Glass System – Solar Absorptance α_S and Emittance ϵ_L Versus Silica Film Thickness (Alumina Crucible)	6-15
6-7	Absorptance of 985 Å Alumina on 730 Å Gold (Polished Aluminum Alloy Substrate)	6-18

Figure		Page
6-8	Absorptance of 1000 Å Silica on 1730 Å Gold (Polished Aluminum Alloy Substrate)	6-18
6-9	Absorptance of 1010 Å Silica on 1040 Å Aluminum (Polished Aluminum Alloy Substrate)	6-19
6-10	Absorptance of 1030 Å Alumina on 740 Å Aluminum (Polished Aluminum Alloy Substrate)	6-19
6-11	Absorptance of 960 Å Alumina on 970 Å Silver (Polished Aluminum Alloy Substrate)	6-20
6-12	Absorptance of 1010 Å Silica on 1450 Å Silver (Polished Aluminum Alloy Substrate)	6-20
6-13	Effect of UV Irradiation on Absorptance; Silica-Silver-Aluminum Alloy System; Substrate at 294° K – 2000 ESH	6-24
6-14	Effect of UV Irradiation on Absorptance; Silica-Silver-Aluminum Alloy System; Substrate at 533° K – 2000 ESH	6-24
6-15	Effect of UV Irradiation on Absorptance; Alumina-Silver-Aluminum Alloy System; Substrate at 294° K – 2000 ESH	6-25
6-16	Effect of UV Irradiation on Absorptance; Alumina-Silver-Aluminum Alloy System; Substrate at 533° K – 2000 ESH	6-25
6-17	Absorptance of OSR	6-26
7-1	Spectral Reflectance of OSR	7-4
7-2	Spectral Reflectance of Alumina-Silver-Aluminum Alloy System	7-5
7-3	Spectral Reflectance of Silica-Silver-Aluminum Alloy System	7-6

TABLES

Table		Page
6-1	Emittance and Absorptance Dependence on Substrate/Surface Quality	6-5
6-2	Effect of Film Thickness on Absorptance and Emittance of Aluminum on Glass Substrates	6-5
6-3	Effect of Film Thickness on Absorptance and Emittance of Aluminum on Polished Aluminum Alloy Substrate	6-7
6-4	Effect of Film Thickness on Absorptance and Emittance of Aluminum on Stainless Steel Substrates	6-7
6-5	Effect of Deposition Rate on Absorptance and Emittance of Aluminum on Glass Substrates	6-9
6-6	Effect of Deposition Rate on Absorptance and Emittance of Silver on Glass Substrates	6-10
6-7	Effect of Deposition Rate on Absorptance and Emittance of Gold on Glass Substrates	6-10
6-8	Results of Screening Test – 250 Equivalent Sun-Hours of Ultraviolet at 533° K – 10 Thermal Cycles	6-21
6-9	Effect of Ultraviolet Irradiation on OSR and Silica/Alumina-Aluminum Alloy Systems – 2000 Sun-Hours of Ultraviolet at 294° K	6-23
6-10	Effect of Ultraviolet Irradiation on OSR and Silica/Alumina-Aluminum Alloy Systems – 2000 Sun-Hours of Ultraviolet at 294° K	6-23
6-11	Optical Characteristics of Selected Coating Systems	6-27
6-12	Calculated Emittance	6-28

NOMENCLATURE

ESH	equivalent sun-hours
OSR	optical solar reflector
A_s	sample area
α_b	receiver absorptance
α_s	solar absorptance
ϵ_H	total hemispherical emittance
ϵ_L	emittance as measured by Lion Emissometer
ϵ_N	normal emittance

Section 1
INTRODUCTION

1.1 OBJECTIVE AND APPROACH

The objective of this program is to investigate techniques and material for finishing spacecraft structural surfaces with reproducible, stable, thermal control materials. Emphasis is placed upon achieving solar absorptance (α_s) values between 0.03 and 0.10 and total hemispherical emittance (ϵ_H) values at room temperature between 0.02 and 0.85. Specific goals are surfaces with (1) an α_s/ϵ ratio less than 0.1, (2) an α_s/ϵ ratio $\doteq$ 1.0 with α_s less than 0.1, and (3) minimum emittance. The resulting surfaces are evaluated for use on spacecraft operating as close as 0.2 AU and at distances of 2.0 AU.

This program required investigations of several coating systems with various substrates. Environmental stability studies and optical property measurements were performed. Vapor deposition equipment was assembled from fabricated parts as well as commercial components. A summary description of the program is given in the following paragraphs.

1.2 COATING SYSTEMS

Experimental methods of producing practical surface systems with low α_s, low ϵ, and low ratios of α_s/ϵ (varying from 2.0 to 0.07) utilizing transparent high-emittance coatings were investigated. Descriptions of the application techniques, including purity of material, deposition rate, pressure, thickness, and substrate temperature, were made.

The specific metals studied were aluminum, silver, and gold.

The specific dielectric materials studied were silicon oxide (vacuum deposited), aluminum oxide (vacuum deposited), and high-purity fused silica.

The following surface systems were investigated:

- α_s/ϵ ratio less than 0.1:OSR-TP-060: silver and fused silica
- α_s/ϵ ratio $\doteq$ 1.0 with α_s less than 0.1: silver and silicon oxide
- Minimum-emittance: aluminum, silver, gold, silicon oxide, and aluminum oxide

1.3 SUBSTRATE REQUIREMENTS

Substrate materials were limited to the following: one selected aluminum alloy, one selected stainless steel, one form of quartz, and one form of glass.

Experimental studies were performed with flat surfaces. In addition, the OSR-TP-060 studies were performed with high L/D cylinders with nominal diameters of 1 in.

Substrate preparation and polishing requirements were evaluated in terms of compatibility with the candidate coating system.

1.4 ENVIRONMENTAL STABILITY STUDIES

The specimens were exposed to simulated solar ultraviolet (UV) radiation. Sample irradiances were 10 "suns" (intensity between 0.2 and 0.35 μ) under high-vacuum conditions (less than 1×10^{-6} torr) using ion pump equipment. The following tests were performed:

- Screening tests with approximately 10-sun UV at 533°K ± 14°K for 250 sun-hours and thermal cycling from 274°K to 422°K 10 times.
- Final tests on selected systems for 2000 sun-hours at temperatures of 294°K and 533°K

1.5 MEASUREMENTS

Measurements of the normal spectral reflectance from 0.27 to 19 μ for the systems selected for final tests were performed before and after exposure.

Solar absorptance (α_s) was calculated from normal spectral reflectance data and the most recent solar spectrum data available.

Total hemispherical emittance was measured as a function of temperature over the range 144°K to 402°K for systems selected for exposure to final environmental tests. Total hemispherical emittance was calculated for these specimens at 294°K, 333°K, 389°K, 444°K, and 555°K from reflectance data and measured at room temperature with the Lion Emissometer.

Section 2
SAMPLE PREPARATION

2.1 OPTICAL SOLAR REFLECTOR

The Optical Solar Reflector (OSR) samples* were prepared by depositing silver upon fused silica substrates, followed by a flash of inconel to inhibit corrosion and protect the back side of the OSR from damage. The fused silica flat substrates were of 0.006 to 0.008 in. thickness, which provides an emittance within approximately 2 percent of the maximum achievable for the bulk material.

The high L/D cylinder was constructed from OSR samples prepared from 0.030-in. thick-walled fused silica tubing. The tubing was cut into 1-in.-long sections and circumferentially sectioned into five equal parts. The cylinder was constructed from a 6-in.-long aluminum tube with a 15/16th-in. outside diameter, such that the final nominal length/diameter ratio was equal to 6.

In all cases the OSR was applied to 6061-T6 aluminum substrates utilizing General Electric RTV-615 silicone adhesive.

2.2 DEPOSITION SUBSTRATES

Substrate material, described in Section 3, was punched from sheet to a 15/16-in. diameter, except for glass substrates which were supplied 1 in. square.

The aluminum alloy substrates were polished directly from the mill surface finish without intermediate sanding or finishing operations. The alloy was polished with a commercial aluminum polish (Met-all).

Substrates were cleaned with acetone, followed by a detergent wash and distilled water rinse.

---

*Supplied by Optical Coating Laboratories, Inc., Santa Rosa, Calif.

Section 3
MATERIAL DESCRIPTION

3.1 VACUUM DEPOSITION SOURCE MATERIAL

The source metals evaporated for low solar absorptance and/or emittance were aluminum, silver, and gold. The dielectric overlays for controlling emittance were silicon dioxide (SiO_2) and aluminum oxide (Al_2O_3).

The form, purity level, and source of the materials were as follows:

- Aluminum

  99.9998-percent purity

  Zone refined

  Cominco 69, pellets (Cominco Products, Inc.)

  Impurities, ppm by weight

Ca	0.1
Cu	0.1
Mg	0.2
Mn	0.2

- Silver

  99.9999-percent purity

  Vacuum melted (electrolyzed)

  Cominco 69, shot

  Impurities, ppm by weight

Bi	0.1	Mg	0.1
Ca	0.1	Si	0.1
Cu	0.1	O_2	2.1
Pb	0.1		

- Gold

  99.9999-percent purity

  Zone refined

  Cominco 69, shot

- Alumina

  Sapphire boules

  Linde-Union Carbide

  Impurities in material to grow crystals, ppm by weight

Mg	2.0	Ga	10
Si	30–60	Cu	<1
Ca	10–20	Ag	<1
Fe	2–5	Cr	Trace
Pb	50–100	Ni	Trace

  Estimated boule purity greater than 99.99999 percent

- Silica

  Quartz chips

  Suprasil

  Englehard Industries

  1 ppm total impurity content

3.2 SUBSTRATES

The substrate materials were aluminum alloy and stainless steel. For controls, glass substrates were used for surface quality reference.

- Aluminum Alloy (Alcoa)

  6061-T6 (1/32 in. thick)

  Condition A mill finish

  Condition B mirror polish

- Stainless Steel

  Type 430

  Republic Steel No. 2

  Bright annealed

  Condition: mill finish (mirror surface)

- Glass

  Corning No. 7059

  Low alkali (less than 0.2 percent)

  Barium aluminum silicate

  Fusion-formed surface

  Typical surface smoothness, 60 Å

3.3 OSR-TP-060

Adhesives and cements were evaluated for use with the OSR. Of special interest and concern was the requirement for service to 500° F. The following 10 adhesives, primers, and cements were selected for evaluation:

- Dow-Corning 93-025 and catalyst (adhesive)
- Dow-Corning 93-033 and catalyst (adhesive)
- Dow-Corning 92-018 (adhesive, one-part)
- Dow-Corning 92-022 (adhesive, one-part)
- Dow-Corning 92-033 (primer)
- Dow-Corning RTV 1200 (primer)
- General Electric RTV 615 and catalyst (adhesive)
- General Electric "Metal Seal," metal-colored silicone rubber (adhesive, one-part)
- LMSC-LP40A, silicate (cement)
- Philadelphia Quartz Kasil 88 (cement)

Epoxy adhesives were not included in the test program because of their nonelastic characteristics.

Section 4
EQUIPMENT AND APPARATUS

The equipment and apparatus used in this investigation include process equipment and instrumentation, environmental test equipment, and optical measurement equipment.

4.1 ELECTRON BEAM VACUUM EVAPORATION SYSTEM

The equipment consists of a basic vacuum system, electron beam multiple-source evaporator and power supply, evaporation rate monitor and controller, ion bombardment system, and evaporation chamber. The integrated electron beam evaporation system is shown in Figs. 4-1 and 4-2.

4.1.1 Vacuum System

An existing 6-in. vacuum system of a nominal 1500 liters/sec capacity and a large-capacity anticreep liquid nitrogen trap was used. A high-vacuum bypass valve was added to permit control of gas pumping during ion bombardment. In a clean condition the system has a base pressure of 4×10^{-8} torr. The system is fail-safe protected.

4.1.2 Electron Beam Unit

The electron beam unit consists of a commercial power supply and gun-crucible assembly.

The power supply (Temescal/EBH-5M3) is rated at 10 kV and 1/2 amp and has a controllable constant power output. The power level can be controlled manually or automatically in conjunction with the evaporation rate controller. The power supply showed excellent operational stability and was more than adequate to meet the requirements of high evaporation rates for aluminum and alumina.

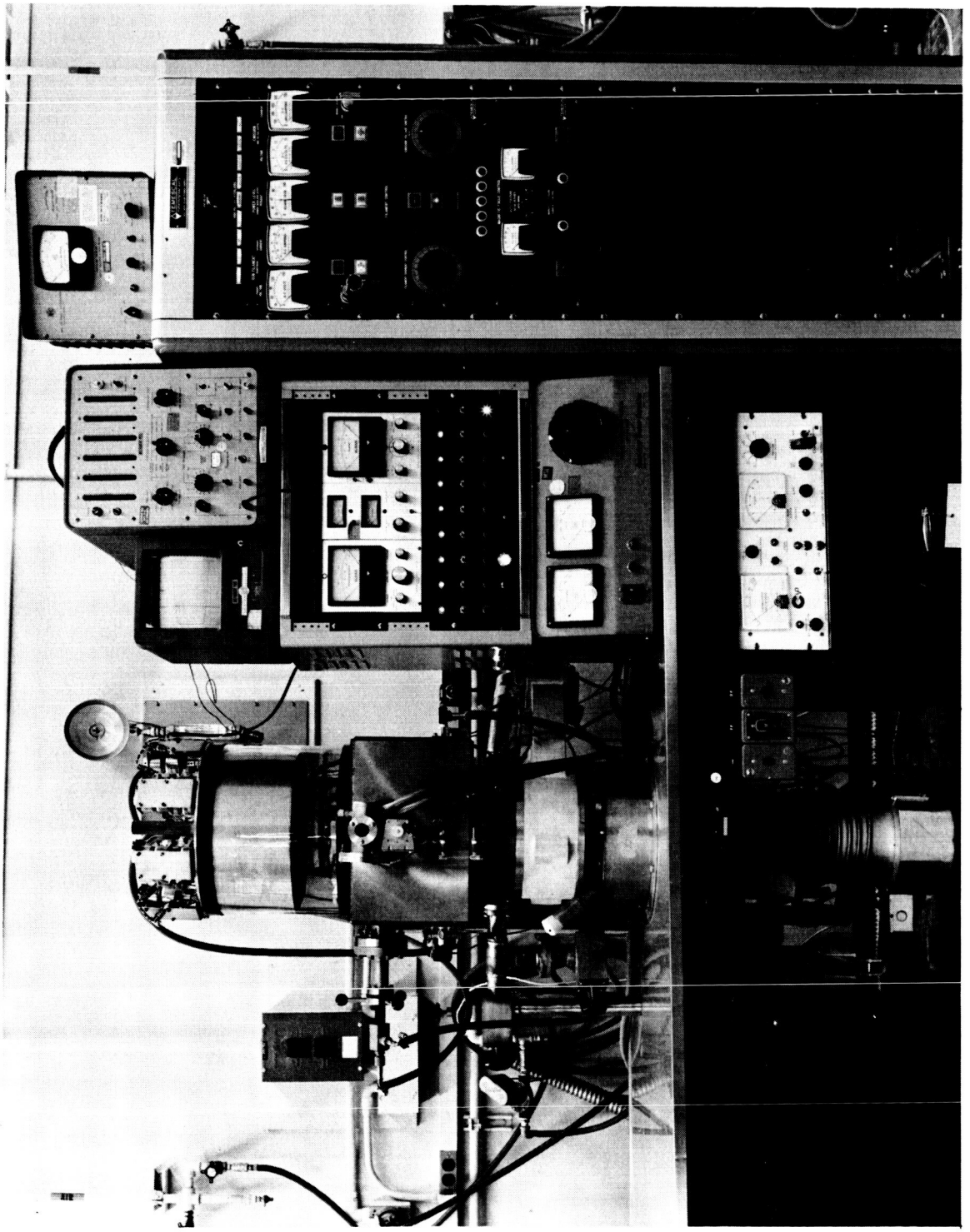

Fig. 4-1 Electron Beam Evaporation System

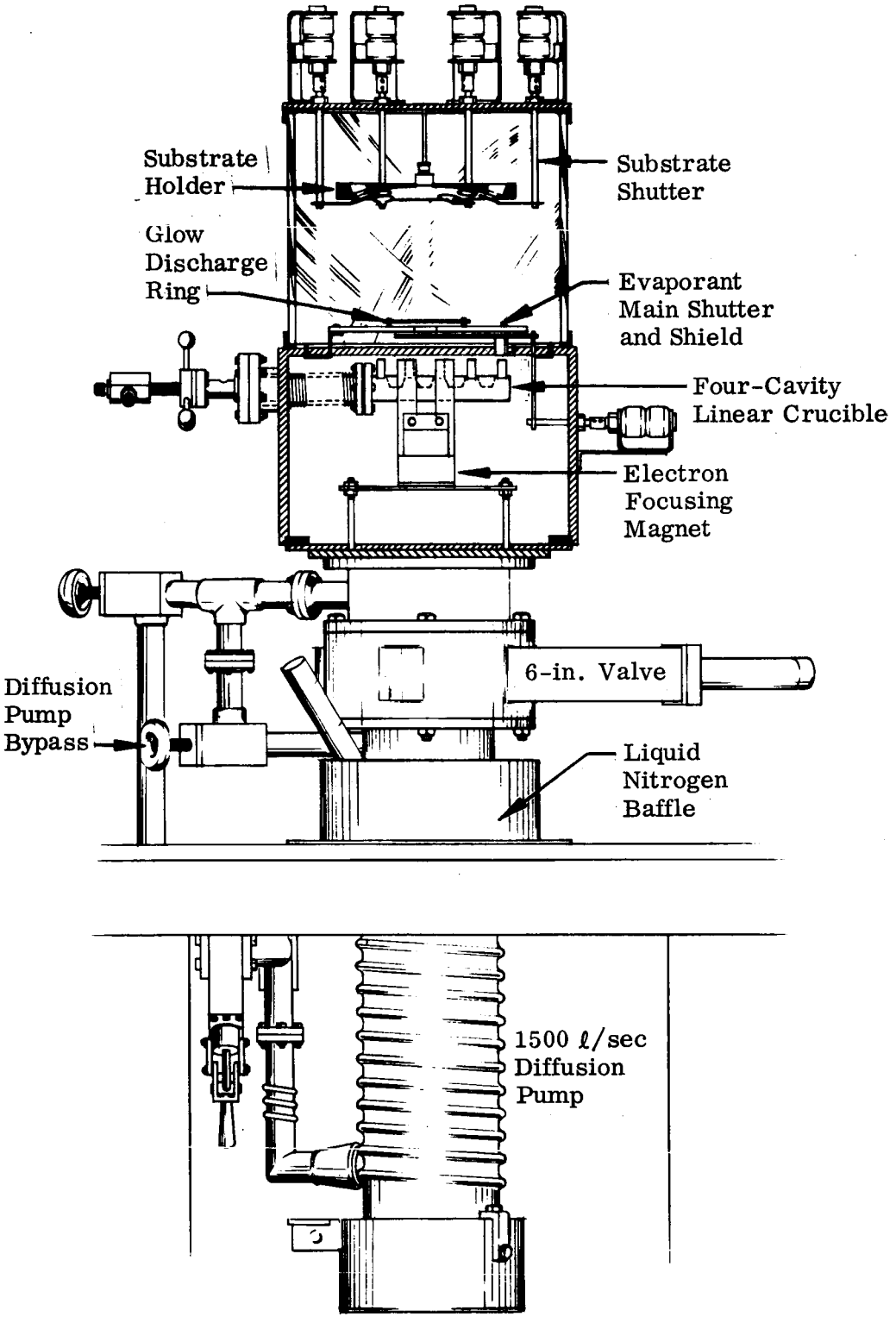

Fig. 4-2 Electron Beam Evaporation System Schematic

The electron beam gun (Temescal 10 LTFH400), shown in Fig. 4-2, consists of an electron emitter and a four-position water-cooled copper crucible, externally positioned, enabling multiple material evaporations during processing.

A modification was made on the electron beam gun. The tantalum hollow anode was replaced with a fabricated water-cooled copper assembly. This change was made for two reasons. First, the electron stream from the tungsten emitter grazes the anode aperture. In evaporation of high-temperature material, such as alumina, the electromagnetic focusing may be changed from the center of the crucible electron impingement to an off-center position in order to deplete the evaporant source uniformly. In so doing, more source electrons strike the anode and may cause evaporation of tantalum, which seriously changes the optical film properties. The second consideration is the probability of reevaporation of high-mobility material, such as silver or its oxides, which have previously been deposited on the anode.

The precautions to be observed in evaporation are discussed in Section 5.

4.1.3 Evaporation Rate Monitor

A commercial rate monitor (Sloan Instruments Omni Model) was used to control film thicknesses of deposition.

4.1.4 Ion Bombardment System

A high-reactance dc supply (Consolidated Vacuum Corp., Model LC-031) was used for glow discharge desorption of the substrate surfaces. The cathode discharge ring and shielded power connector were fabricated as part of the baffle and main shutter assembly. The ring and shield were fabricated of commercially pure aluminum to minimize sputtering.

4.1.5 Evaporation Chamber

The evaporation chamber includes a ground stainless steel box, a 14-in. Pyrex cylinder, and a top flange to which the substrate holder is attached. The steel chamber

contains the evaporator, ion bombardment electrode and source shutter assembly, and high-voltage and water circuit lead-throughs. The substrate holder (Fig. 4-3) provides eight substrate positions. This holder is readily removed from the upper Pyrex cylinder flange for ease in changing substrates. The quartz crystal transducer is mounted to the center of a spherical stainless steel flange. The crystal is mounted on a water-cooled dispenser changer (Sloan) enabling change of crystal during operation.

Temperature monitoring of the substrate is accomplished with a thermocouple spring loaded to the back surface of the substrate.

Each substrate position is independently shuttered. The shutters are actuated by bidirectional motors, remotely controlled, which enable depositions of varying film thicknesses while maintaining deposition parameters constant. The shutter drives are mounted to the upper support structure (Fig. 4-4).

4.2 OPTICAL MEASUREMENT EQUIPMENT

4.2.1 LMSC Low-Temperature Emittance Apparatus

The LMSC low temperature emittance apparatus is shown in Figs. 4-5 and 4-6. (Ref. 2). This apparatus is used to determine the emittance of materials in the temperature range from 70°K to 400°K, utilizing the boiling point of liquid hydrogen as a ground temperature. The heart of the apparatus consists of a 2-1/2 inch diameter aluminum sample substrate to which has been bonded the material whose emittance is to be determined. The sample or radiator faces a black-body of the same diameter. The black-body consists of an array of aluminum tubes. The interior of the black-body has been coated with a flat black paint.

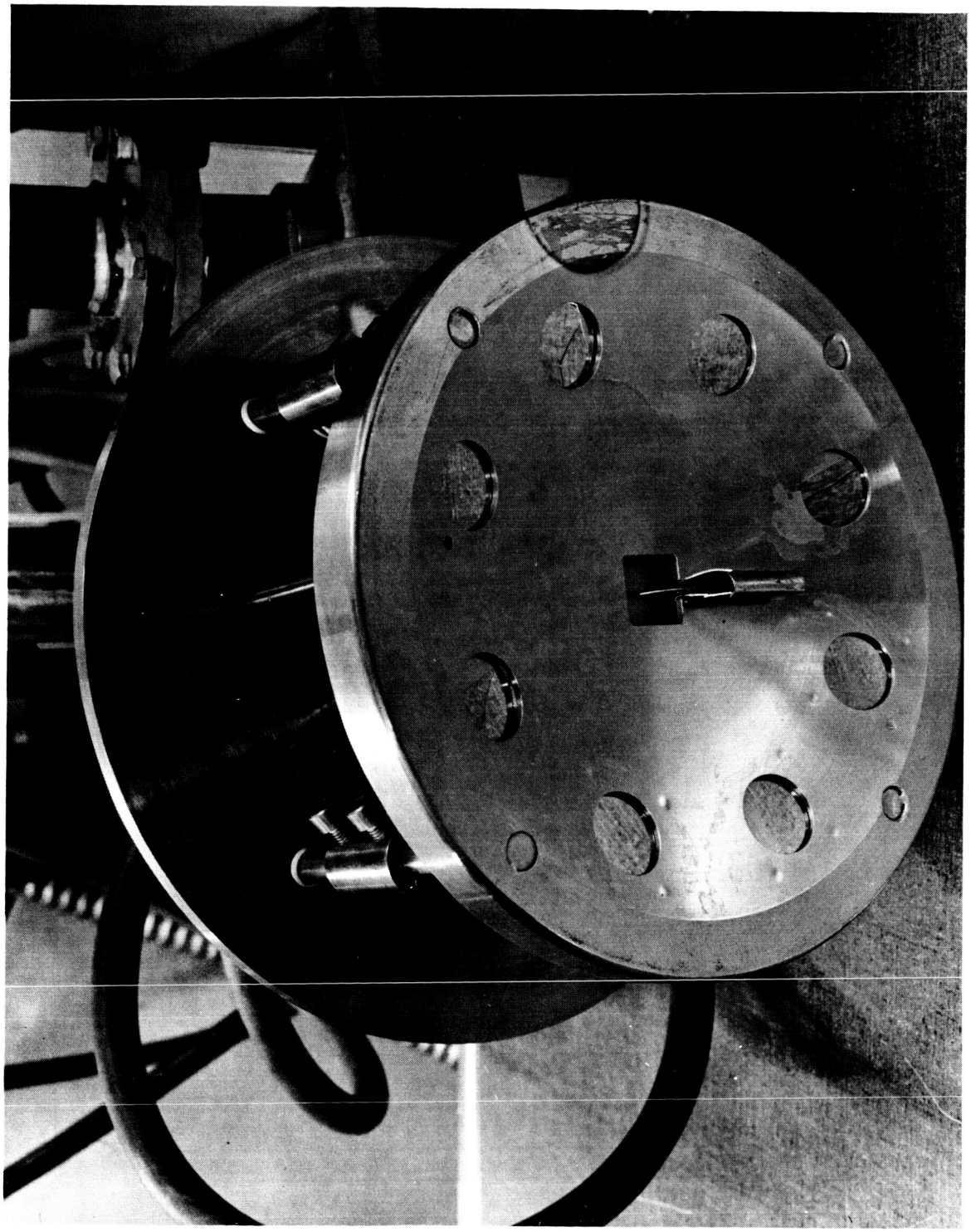

Fig. 4-3 Substrate Holder

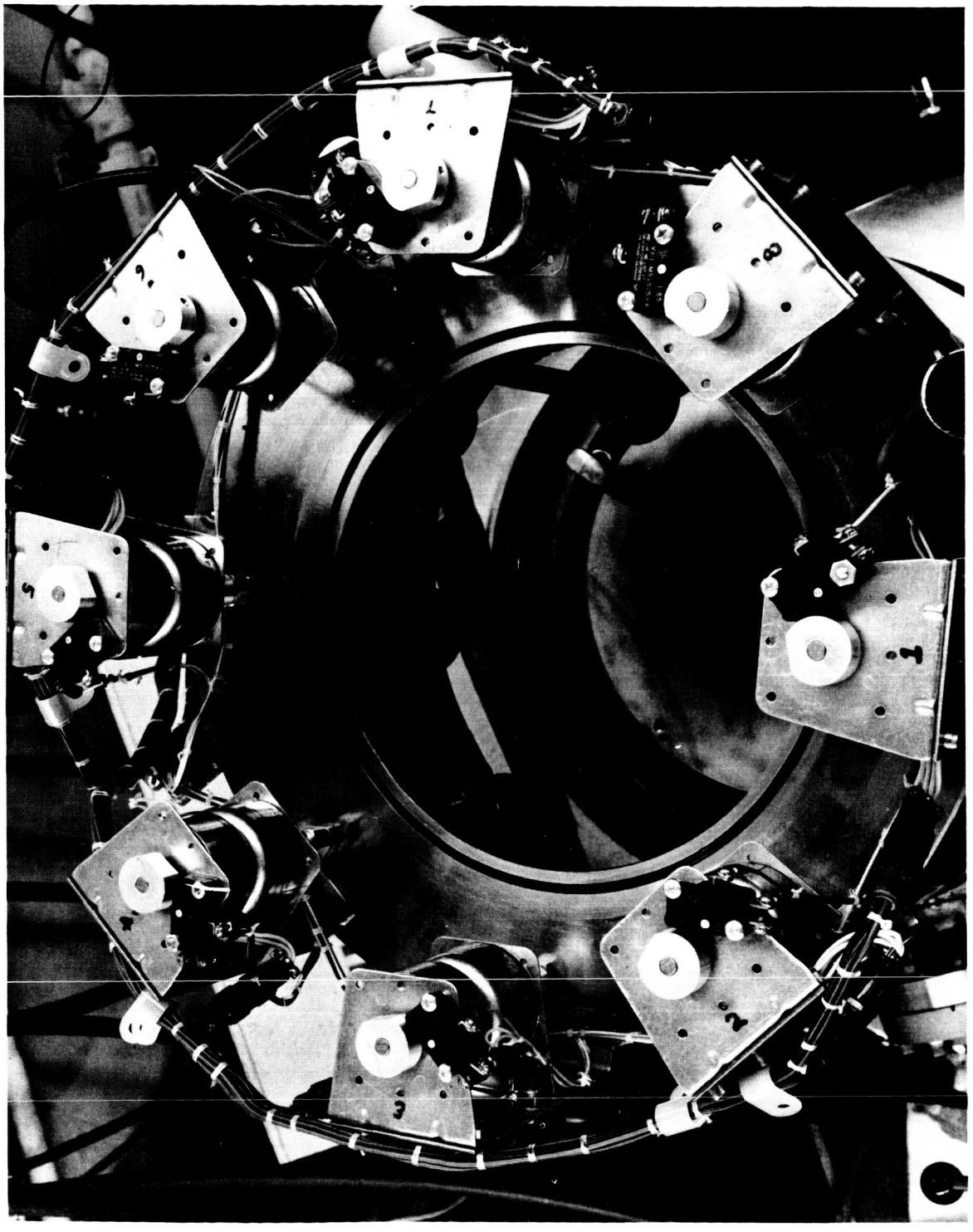

Fig. 4-4 Upper Support Structure

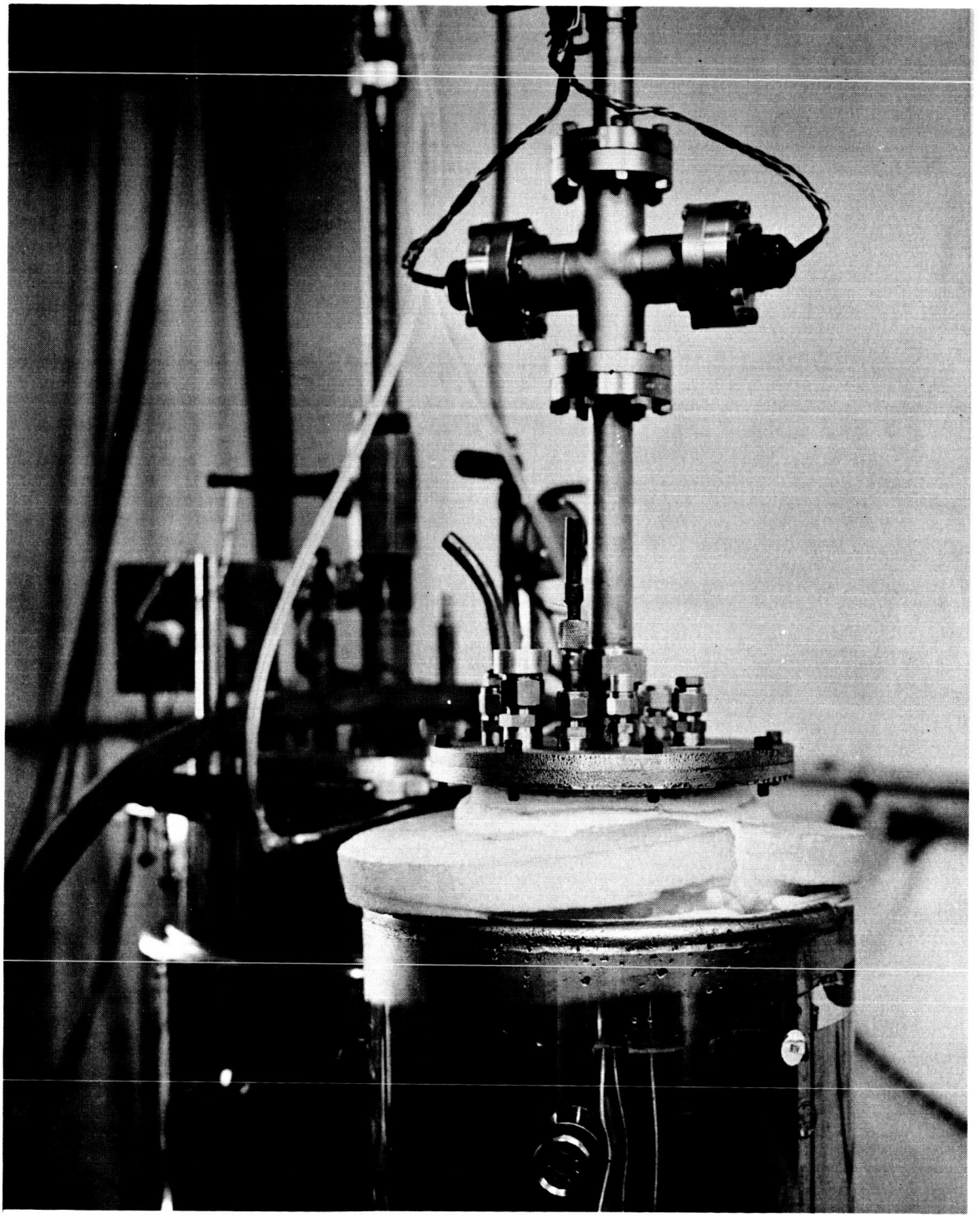

Fig. 4-5 Low-Temperature Emittance Apparatus

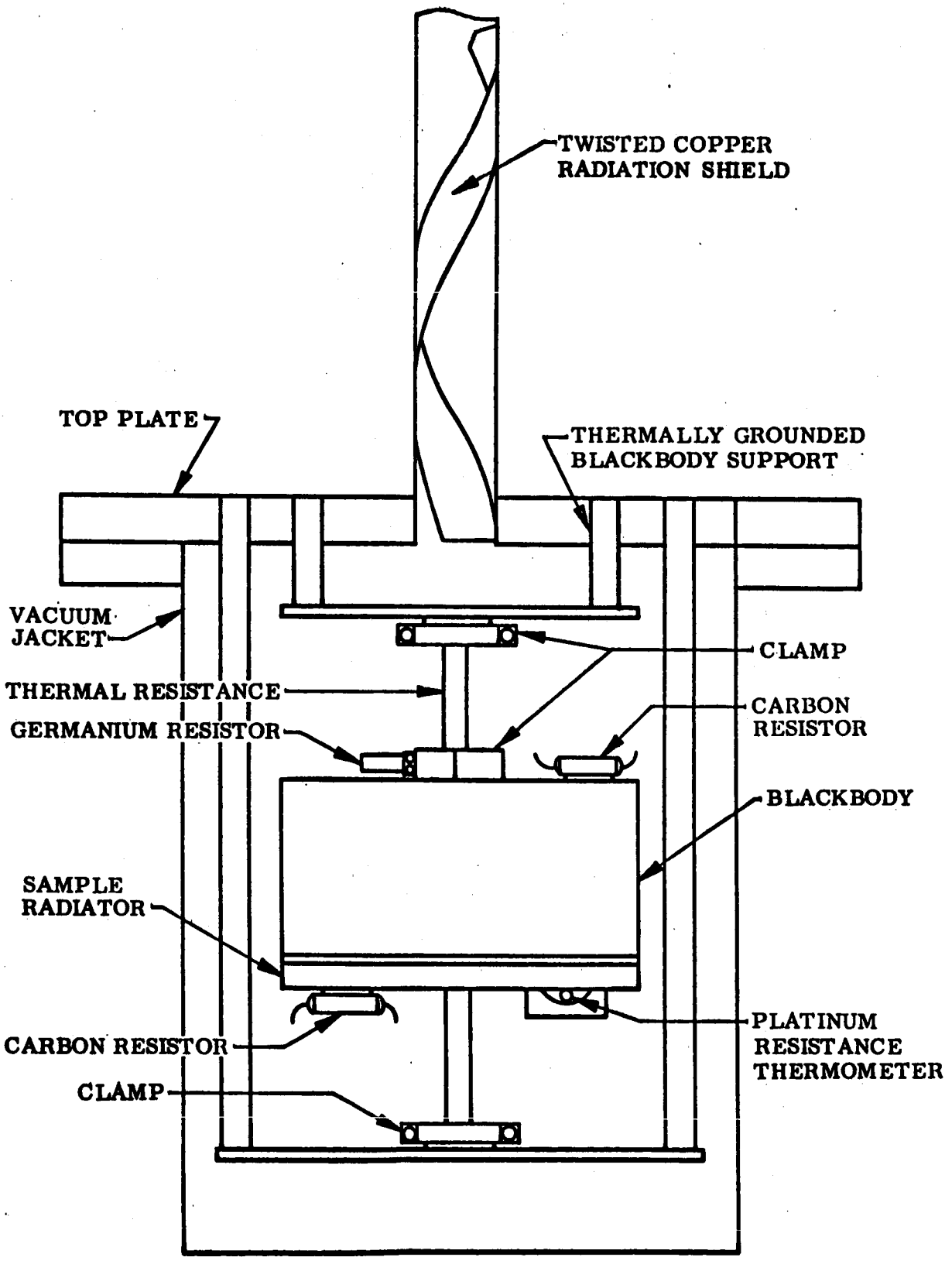

Fig. 4-6 Schematic of Low-Temperature Emittance Apparatus

By providing both the sample radiator and black-body receiver with a heater and a thermometer, the emittance measurements can be made. The black-body is heated during sample runs by the radiation from the front face of the sample. By noting the temperature of the black-body during sample runs, the radiant energy emitted by the sample can be calculated by calibrating the black-body receiver (Figs. 4-7 and 4-8). During calibration, the black-body is heated with its own heater (a carbon resistor) to the same temperature as in the sample runs and the power dissipated in the carbon resistor is noted. The emittance has a maximum error of 3 percent in the temperature range of 60°K to 300°K and 1 percent at room temperature.

4.2.2 Cary Model 14 Spectrophotometer

Spectral normal reflectance measurements in the spectral range from 0.275 to 1.8 μ are made with an Applied Physics Corporation Cary integrating-sphere spectroflectometer. This instrument uses the well-established integrating sphere technique as adapted to a double-beam automatic ratio recording spectrophotometer. From the measurements obtained with this instrument, the solar absorptance is determined.

In operation, a test sample is placed at one sphere opening and a reflectance standard is placed at the reference beam location. The instrument is calibrated in such a manner that the ratio of signal levels from the sample and standard are automatically recorded in terms of absolute sample reflectance. The standards used for calibration are first surface aluminized mirrors which are carefully prepared from 99.999-percent purity aluminum by vacuum deposition in this laboratory.

4.2.3 Lion Optical Surface Comparator

The total hemispherical emittance is measured using the emissometer portion of the Lion Research Corporation Optical Surface Comparator. This instrument measures the emittance of the sample surface at room temperature. This device works on a comparative principle in that the surface of interest is compared to known reference standards. The detector of the emissometer head views an area on the test surface about 1 in. in diameter. Energy emitted by the surface is sensed through a KRS-5

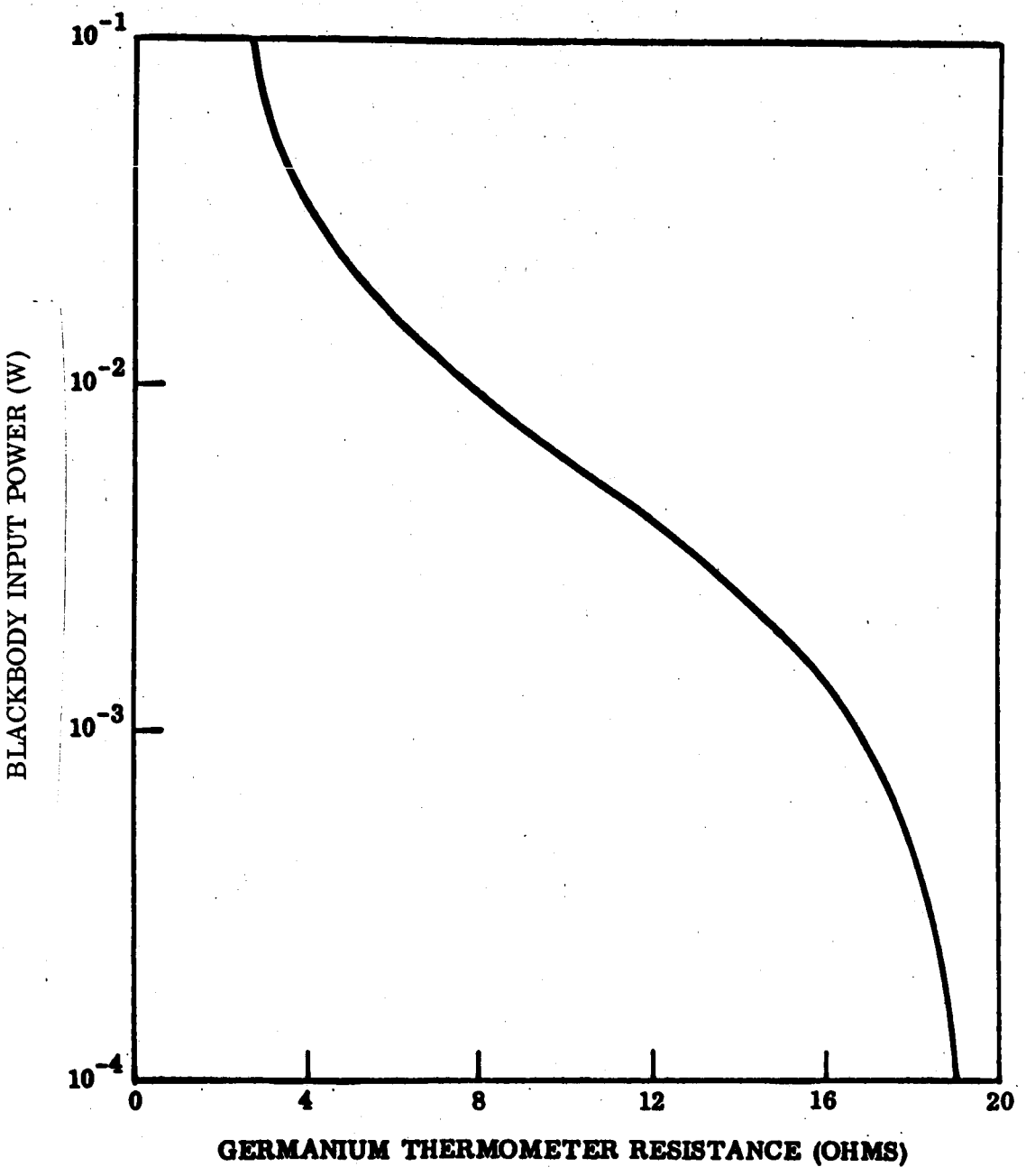

Fig. 4-7 Blackbody Receiver Calibration Curve

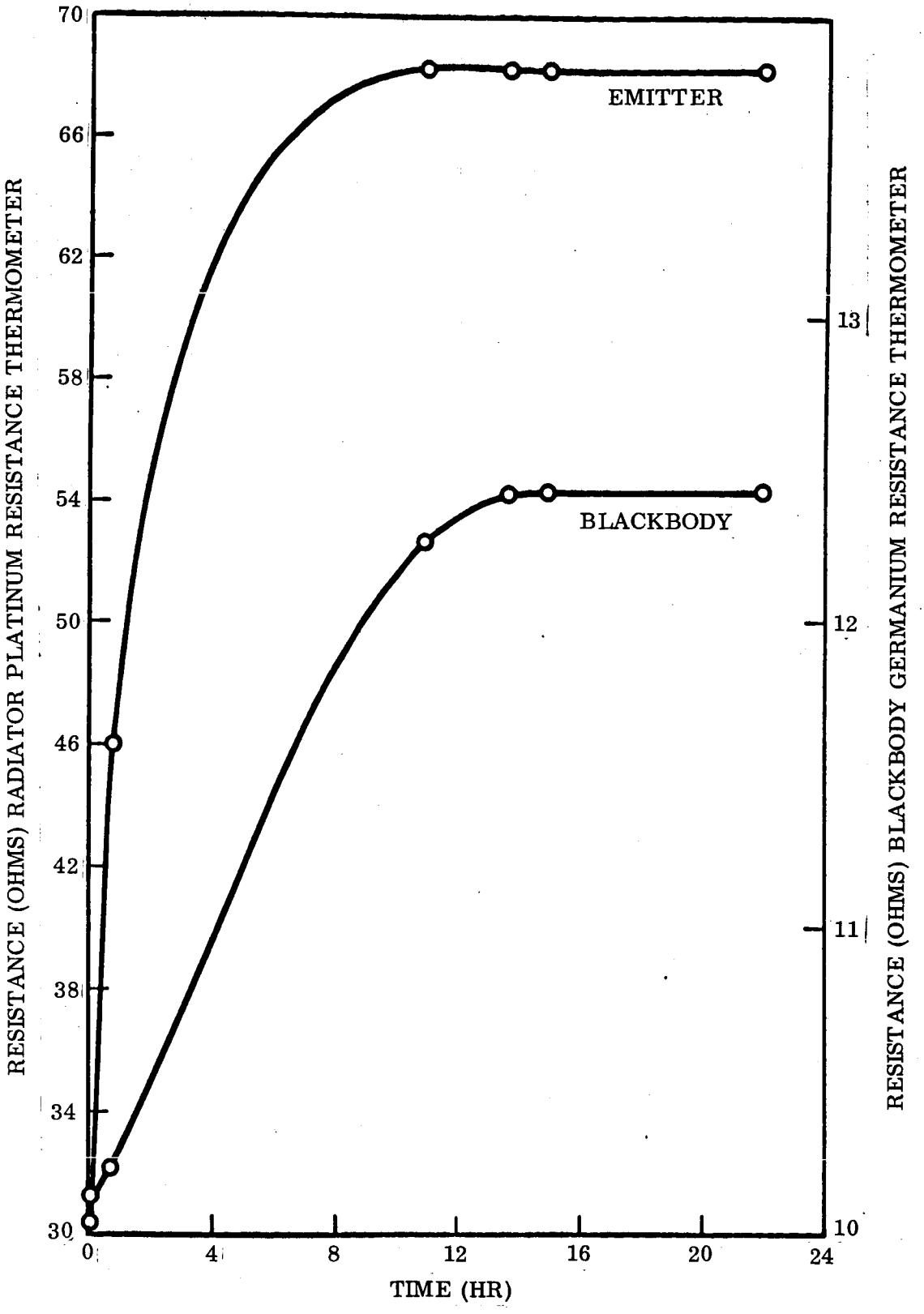

Fig. 4-8 Typical Time Required To Attain Radiator and Receiver Temperature Equilibrium

infrared window with a thermoelectrically cooled (~ 0°F) thermopile mounted in an evacuated chamber. Before the specimen to be measured is viewed, the energy emitted by three standards (ϵ = 0.03, 0.48, 0.85) is detected and the thermopile is calibrated.

4.3 ENVIRONMENTAL TEST EQUIPMENT

The static ultraviolet exposure chamber is shown in Fig. 4-9. The test chamber is a water-cooled stainless steel bell jar 14 in. high and 14 in. in diameter. The 1-in.-diameter samples are mounted on a water-cooled, semicylinder copper sample holder concentric with the ultraviolet source and at a distance which results in nominal irradiances of 10 suns of ultraviolet energy. A flux density of 1 sun of ultraviolet energy is herein defined as the flux density of extraterrestrial radiation at 1 AU from the sun, in the wavelength interval from 2000 to 3500 Å. At these flux densities the sample temperatures were maintained between 294° K and 533° K for all ultraviolet tests in this chamber. Thermal contact conductance between the sample and the water-cooled copper sample holder was controlled by means of individual mounting frames which pressed the backface of the sample against the copper. Vacuums are established prior to initiation of ultraviolet exposure with cryogenic sorption roughing pumps and an electronic high vacuum pump to prevent the possibility of oil contamination. The chamber pressure is typically 2×10^{-7} torr in the last portion of an exposure period and before the lamp is started. At the beginning of the exposure period, the pressure typically rises to 5×10^{-7} torr.

The source of ultraviolet energy is a 1 kW AH-6 (PEK Labs Type C) high-pressure mercury-argon capillary arc lamp. Approximately 35 percent of the radiant output of the lamp is in the interval from 2000 Å to 4000 Å; the total output is in the interval from 2000 Å to 26,000 Å. The lamp is water cooled and has a quartz water jacket and velocity tube. This assembly is lowered into a quartz envelope extended into the exposure chamber from the top. The assembly can be withdrawn to change lamps

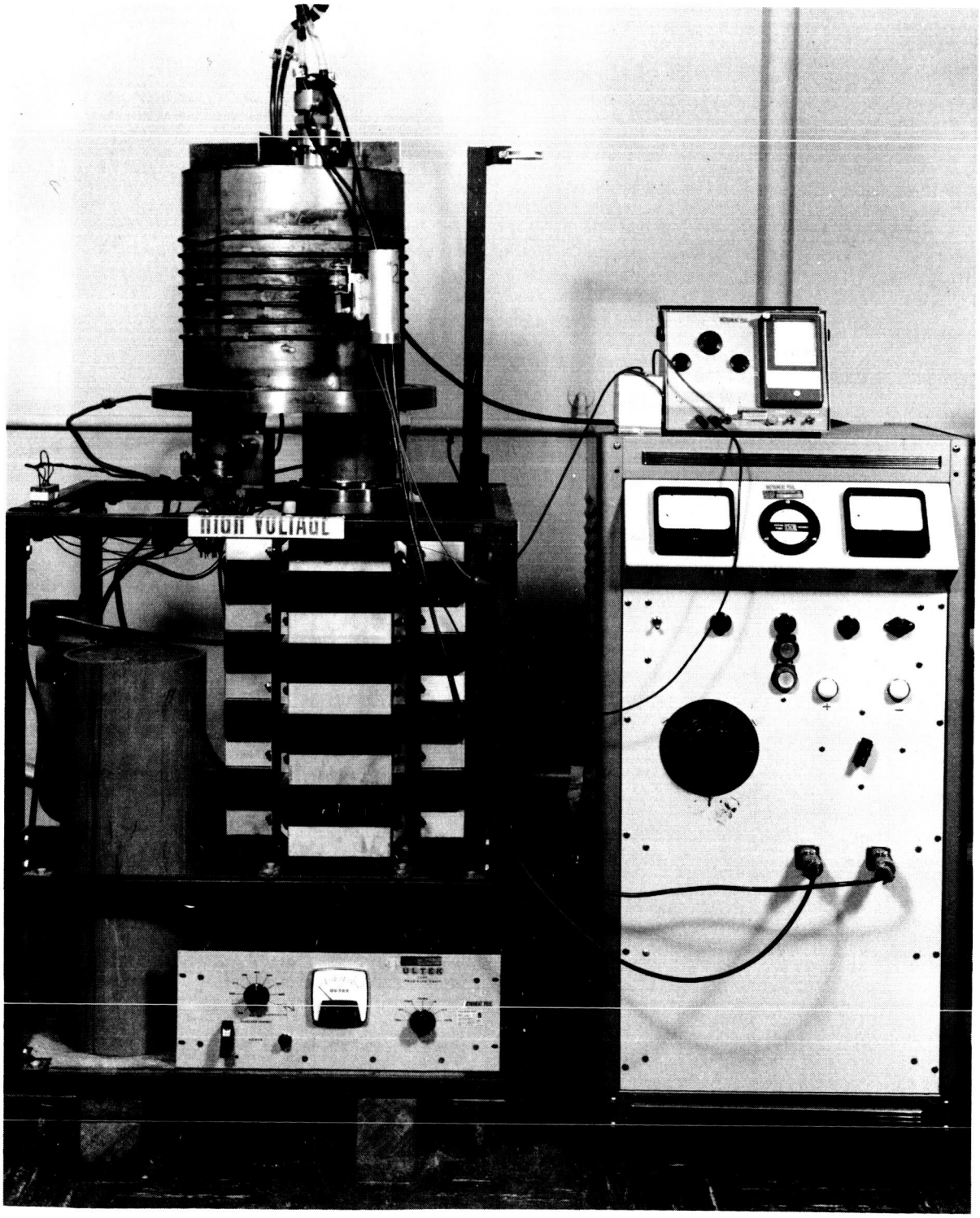

Fig. 4-9 Ultraviolet Radiation-High Vacuum Exposure Apparatus

without disturbing the established vacuum. Unless a lamp ruptures, it is run for 100 hr and then replaced. Each test is begun with a new lamp. This procedure is followed because the AH-6 output decreases more in the 2000 Å to 3000 Å interval than in the 3000 Å to 4000 Å interval. Therefore, for materials which are degraded primarily by energy of wavelengths less than 3000 Å, an old lamp will produce less degradation than a new lamp for the same total ultraviolet exposure, expressed in sun-hours. Some control over this effect is achieved by following this standard replacement procedure.

The ultraviolet intensity is monitored external to the vacuum chamber with a calibrated RCA-935 phototube in conjunction with a Corning 7-54 filter, which transmits only the near-ultraviolet output of the lamp. The output of the phototube is automatically measured and recorded for a few minutes each hour with a recording microammeter. The intervening quartz window and 7-54 filter are periodically checked for degradation in spectral transmittance and cleaned or replaced as necessary. When desired, a Corning 0-54 filter is used to compare the intensity in the 2000 Å to 3000 Å region to that in the 3000 Å to 4000 Å region as a measure of the relative degradation of lamp output in the shorter wavelength regions.

Section 5
EXPERIMENTAL PROCEDURES

5.1 OSR PROCEDURE

Evaluation of the adhesives to be used with OSR-TP-060 preliminary screening tests consisted of applying OSR-TP-060 segments to 6061-T6 aluminum substrates. Flat substrates were used, but the suitability of the adhesive for application to 1-in. cylinders was observed. The cured specimens were inspected for corrosion. They were heated to 533°K and thermally cycled between 533°K and room temperature. These preliminary thermal cycling tests were performed at atmospheric pressure. Thermal cycling tests with the more promising candidate adhesives were performed in a vacuum, and the final environmental stability tests included ultraviolet radiation. The equipment and apparatus for the environmental studies were described in Section 4.

5.2 DEPOSITED OPTICAL FILMS

The program objective was the investigation of techniques and material for application of optical coatings for thermal control of spacecraft structural surfaces. Concomitant with the objective of specific optical properties is the selection of appropriate coating systems that have engineering practicality. To accomplish this objective, the coating systems must be thermally stable and reproducible and must have minor degradation when irradiated in vacuum with ultraviolet.

To stay within the confines of the contract objectives, the coating systems investigated were logically selected on the basis of the desired optical characteristics of the coatings and the mechanical properties of the substrate materials.

A vapor deposition process has a large number of variables.* Large morphological changes can result from small changes in process variables. The equipment was

*(Refs. 3, 4, 5, and 6).

designed to permit evaluation of these process variables. The vapor stream, from evaporation source to substrate, was remotely controlled by eight independent substrate shutters, as well as the main source shutter to permit maintaining of constant evaporation conditions while controlling deposition thickness or deposition sequence. The major kinetic process variables controlling the optical characteristics are deposition rate and thickness, substrate temperature, source temperature, system pressure, and nature of the residual gas. The effects of nonkinetic process parameters are discussed in Section 7.

5.2.1 Assembly, Instrumentation, and Checkout

The vapor deposition system (Section 4) was checked out for performance. Materials of interest were evaporated on glass substrates in order to calibrate the quartz transducer of the Sloan rate monitor. The deposited materials calibrated were aluminum, gold, silver, silica, and alumina.

The rate monitor showed good reproducibility of mass change from crystal to crystal, as would be expected inasmuch as the absolute value of resonant frequency is not as important as the frequency shift due to mass addition to the quartz crystal. The rate monitor is easily used and accurate within 4 percent for films of the order of 500 Å, 2 percent for films of the order of 1000 Å, and 1 percent up to 10,000 Å. Statements of film thicknesses of approximately 200 Å or less are of little significance for most deposits. The weight per unit is a more accurate representation.

The accuracies indicated apply only if certain precautions are observed. The accuracy and response (frequency shift output stability) are valid if the deposits on the quartz crystal are compatible and do not become thicker than indicated by a frequency shift of the order of 100,000 Hz. Inaccuracies will increase as thicker depositions occur on the quartz crystals. Attempts to monitor thin films (of the order of 500 Å) with a crystal that has been previously coated with thick films will result in inaccuracy. Additional causes of inaccuracy were thermal shock to the quartz crystal and

incompatible depositions on the crystal. Deposits that are highly stressed or that have poor adhesion (such as silica and gold) are likely to cause nonlinear frequency shifts as the resonant frequency of the quartz crystal shifts. The reason for this may be that the deposited films cause asynchronous oscillations.

The frequency shifts were measured with a counter using a 1-sec summing interval. This was very satisfactory and enabled reading to ± 1 Hz. Control of thin-film thickness at high evaporation rates (1000 Å/sec) is difficult because of shutter response time.

The absolute film thickness was measured by conventional optical interferometric methods (Hilger and Watts). The method of fringes of equal chromatic order was used. The accuracy of this method with the instrument used is within 10 Å in the nominal range of 0 to 5000 Å. This would be true only under highly idealized conditions and after many laborious and "interpretive" measurements. In practice, the accuracy of this method for measuring films below 100 Å is questionable unless optically flat substrates are employed: Also, providing these surfaces are single crystal or amorphous (crystallites of the order of 20 Å). This further assumes that there is such a thing as a "film" of 100 Å thickness – which is a matter for the philosopher to decide. Electron micrographs do not show a film continuum in this range of mass deposition. (Ref. 7). For ease in discussion and indication of order of magnitude, film thicknesses stated in this range are, in fact, only inferred from mass and do not represent a real morphological state.

The glass substrates used for calibration were made of specially drawn smooth glass of 60 Å typical surface smoothness. The wave contours of this glass were of the order of 200 Å at approximately the same pitch as the film step width. This limited the minimum absolute thickness determination to about 250 Å.

Film thicknesses up to 2 μ can be measured by tapering the film step, which is done by spacing the mask from the substrate by 1/32 in. This results in a wide film step, permitting observation of fringe displacement on the interferometric microscope.

The results of the film thickness monitor calibration show the following film densities compared with gold, (used as the reference because of the ease of depositing films with density nearly that of bulk).

	Gold	Silver	Aluminum	Alumina	Silica
Bulk Density	19.3	10.5	2.7	3.6	2.1
Inferred Density (from frequency shift of quartz crystal)	–	10.5	2.86	3.2	2.1

These values were obtained by averaging the frequency shift per angstrom of film thickness for film thicknesses ranging from 300 Å to 15,000 Å.

Aluminum showed higher density than bulk, which is explained in part by the fact that the oxide forming on the aluminum has a higher density. In thin films, the oxide formation may be 5 percent of the film thickness.

Alumina shows a lower density than bulk. This is due in part to some contamination resulting from the use of a composite crucible (boron nitride-titanium diboride mixture; use of this crucible was discontinued in favor of evaporation of sapphire (Al_2O_3) boules directly from the water-cooled cavity of the electron beam gun crucible.

The rate monitor counter showed the following frequency shifts for the materials of interest:

Material	Hz/Å
Gold	13.6
Silver	7.4
Aluminum	2.0
Alumina	2.2
Silica	1.5

It should be noted that these values are valid only for the system geometry and the evaporation conditions. Variations in evaporation conditions that cause deviations of the film density or use of different substrate materials and surfaces can result in an inferred film thickness that is grossly in error. Not only may the deposition on the quartz transducer be different from the simultaneous deposition on the substrate of interest, but the deposition on the quartz transducers may also be variable from run to run even though the mass change indicated is constant. These potential sources of inaccuracy are minimized by frequent changing of the quartz transducer.

The materials of deposition have high accommodation with the quartz transducer and substrate materials. The inferred thickness of the substrate film is, therefore, equal to the actual film thickness of the monitor transducer.

5.2.2 Processing of Optical Coatings

The processing of the optical coatings was accomplished in a conventional manner. After equipment checkout and instrument verification, routine depositions were made on glass substrates with the various evaporants of interest in order to establish which operational parameters were critical. The principal kinetic processing parameters affecting absorptance were primarily deposition rate and deposition thickness. Depositions were made on various substrates of interest with metals and dielectrics under investigation.

A typical deposition sequence was as follows:

- Evaporation crucibles were loaded with desired evaporant materials. Eight substrates, after preparation, were loaded onto the substrate holder, and the monitor thermocouple was placed on the back of a substrate.
- The substrate holder was then placed on the upper mounting flange. The system was pumped by a mechanical pump to 100 μ or less. The liquid nitrogen baffle was filled, and the main gate valve was opened. After the pressure in the chamber was in the 10^{-7} torr range (of the order of 3 min), the main vacuum valve gate was closed and oxygen leaked into the deposition chamber with the roughing pump valve open until a pressure of 50 μ was reached and maintained.

- Substrates were bombarded with O_2 ions at 1000 Vdc and 200–300 mA for 2 min. The roughing valve was closed and the diffusion pump bypass valve was opened. The O_2 leak was adjusted for a 20-μ system pressure.
- Ion bombardment was continued for 30 to 60 sec with approximately 1500 V and 100 mA. The gas discharge supply and oxygen leak were turned off and the main gate opened to the pump evaporation chamber.
- Substrate temperature rise was from room temperature to approximately 310°K.
- Cooling water was turned on to the anode circuit, crystal detector holder, and copper crucible block.
- Emitter filament voltage and electron magnetic focusing coil voltage were applied.
- With the power level set at zero and the high voltage control set at approximately 30%, the high voltage was turned on. The power level was raised until electron impingement was observed. The electron beam was then steered to the center of the crucible.

The evaporant was outgassed at a low power level, and the source shutter was closed. The amount of outgassing was very small with the high-purity vacuum-melted source materials used. The proper voltage and power level setting for each material and desired evaporation rate was determined empirically.

When the desired evaporation rate was stable, the main shutter was opened and deposition was made on appropriate substrates as selected by substrate shutters. When a frequency shift representative of the desired film thickness was reached, the main shutter was closed or individual substrate shutters were closed, dependent upon the desired film thicknesses. This was repeated for other evaporation materials by translating the water-cooled crucible block to another desired material crucible position.

At termination of deposition, the shutter was closed and the evaporation power supply was turned off. When the source material had cooled, the system was opened to the atmosphere and substrates were removed.

5.2.3 Environmental Testing of Optical Surfaces

Prepared samples were mounted on a sample holder, and the test described in Section 4 was performed. The ultraviolet irradiation was accelerated by a factor of 10, in the 2000–3500 Å wavelength region, with reference to the extraterrestrial solar spectrum. The screening tests were made for 250 sun-hours with substrates at 533°K plus 10 thermal cycles between 300° and 533°K. Selected optical systems were then tested for 2000 ESH with substrates at 294° and 533°K.

5.2.4 Optical Measurements of Coatings Before and After Irradiation

The following optical measurements were made on the equipment described in Section 4.

- Emittance using the Lion Optical Surface Comparator (ϵ_L).
- Spectral reflectance measured from 0.275 to 1.8 μ on the Cary Spectrophotometer. Solar absorptance was calculated from the integration of the Cary trace, which is adjusted for variations in solar flux at various wavelengths.
- Low-temperature total hemispherical emittance samples were mounted in the low-temperature emittance apparatus described in Section 4. Measurements were made at temperatures of 105° to 402°K.

Directional spectral reflectance properties were measured over the spectral range of 2 to 25 μ with a Gier Dunkle Heated Cavity Absolute Reflectometer. The measurements were performed with samples prepared on 1-in.-diameter aluminum discs. Spectral reflectance at a polar angle of 15 deg was measured for samples prior to and following environmental exposures. Normal emittance was calculated by integrating the reflectance data with respect to the corresponding blackbody distribution at 294°, 333°, 389°, 444°, and 555°K.

Section 6
EXPERIMENTAL RESULTS

6.1 OSR ADHESIVE EVALUATION

A program to select an adhesive for bonding the OSR to aluminum substrates was successfully completed. Classes of adhesives considered during the program included epoxies, polyesters, polystyrenes, and silicones. Of these classes, the silicone adhesives provided the most desirable characteristics for use with the OSR. Of the silicone adhesives tested, General Electric RTV-615 exhibited the most desirable properties, performing satisfactorily in all the environmental tests. RTV-615 is relatively easy to apply and has desirable curing features.

The substrate material of primary interest during the investigation was bare 6061 aluminum. The environmental tests were performed using bare aluminum as a substrate material, and the selection of RTV-615 was based on its ability to bond the OSR to bare aluminum substrates.

For applying the OSR to flat and curved substrates, the following characteristics are desirable of the adhesive:

- Adequate bonding capabilities
- Elastic over the required temperature range
- Noncorrosive to silver
- Relatively long pot life, especially in a thin film state
- Room-temperature curing
- Free from residual stresses upon curing
- Relatively small shrinkage upon curing
- Easy to apply to uniform film thickness of 2 to 3 mils
- Ability to maintain good bond through room temperature to 500°F thermal cycling

The 10 candidate adhesives listed in subsection 3.3 were evaluated in terms of the desirable characteristics listed above. Where recommended by the manufacturers, the adhesives were applied to primed substrates. Primer was not applied to the OSR surfaces. The results are qualitative and represent relative judgments based on comparison of one adhesive with another.

Corrosion of the silver was noted on various OSR samples with several cements. No attempt was made to determine the exact cause of silver corrosion when these adhesives were used. When tested as cements for use with OSR-TP-060, LP40A, and Kasil 88 proved to be noncorrosive and to have good adhesion. However, the lack of elasticity and poor cohesive strength resulted in failures due to thermal stresses under thermal cycling. The preliminary tests indicate that these inorganic cements are unsatisfactory for use in this program.

The one-part adhesives, Dow Corning 92-018, Dow Corning 92-022, and General Electric "Metal Seal" caused no corrosion, and their high viscosity makes them suitable for application to cylinders. Techniques were devised to apply a thin layer of uniform thickness to cylinders and flat surfaces, but some separation occurred at the bonding surfaces of the OSR upon heating. This separation was apparently due to nonuniform dimensional changes in the silicone (probably) related to shrinkage on curing). For Dow Corning 92-018 and General Electric "Metal Seal," the separation occurred at approximately 422° K. For Dow Corning 92-022, the separation occurred at an indicated furnace temperature of 500° K. Curing the one-part adhesives did not seem to be a problem, but their performance at elevated temperatures was marginal at best.

It is important to note that no corrosion was detected when RTV-615 was used, and RTV-615 was the only adhesive evaluated that met all the requirements established for bonding the OSR to aluminum substrates.

6.2 DEPOSITED COATING SYSTEMS

The results of the preparation, processing, environmental testing, and optical measurements are presented in three major parts:

- Coating system parameters
- Optical characteristics
- Ultraviolet environmental test results and optical measurements

The interrelationships and their interpretation are considered in Section 7.

6.2.1 Coating System Parameters

These parameters are artificially separated into kinetic and passive parameters for convenience in discussion. In actuality, these interrelationships may, and often are, highly nonlinear and synergistic for many coating systems.

6.2.2 Passive Deposition Parameters

The passive deposition parameters are:

- Substrate topography
- Substrate surface quality
- Substrate material
- Substrate cleanliness
- Evaporant source purity
- Source cleanliness
- System cleanliness
- Impingement angle of incidence

The effects of these parameters on the mechanical, electrical, and optical properties are well understood in general terms. However, in relation to a particular program, it is generally impractical to specify categorically the quality of optical films in terms of a limited number of parameters. Rather, it is essential first to establish objectives which are compatible with the scope of the program, and then to attempt to accommodate these goals within the parameter limits. This is usually prescribed by

economic considerations. The difficulty lies in ascribing suitable bandwidths to the parameters such that a presumed parameter does not become an independent variable when another presumed parameter approaches its allowed limits (which may be arbitrary).

The complexity of the surface chemistry of the substrates is one of many dominant factors in assessing the deposition parameters. To stay within the scope of the investigation, certain conditions were arbitrarily established, based primarily on engineering practicability and on the end use of the thermal-control coating system. Although a complete cataloging of a wide range of materials of various surface finishes would be desirable, the scope of the program strongly dictated the character of the selected systems. The substrate materials selected (Section 2) are stock materials readily available. The area of subjective evaluation is in the surface quality of the polished aluminum alloy substrate. With this exception, the substrate material, topography, and quality are established.

Liberties can be taken with optical surfaces that are used for thermal control that would not be permitted in other applications. For example, "pin holes" and some scratches, although not aesthetically pleasing, have a very small effect on the optical absorptance or emittance. On an area basis, they are insignificant.

Gross surface roughness affects surface emittance, whereas small surface roughness (crystalline as compared with amorphous) can cause large changes in solar absorptance. (See Table 6-1.) In the case of a polycrystalline surface, the size of the crystallites is important. This is shown in the case of the alloying additions in 6061 aluminum alloy. The heterogeneous crystalline aggregate structure presents preferred sites for aluminum deposition to form in large agglomerations. This results in a significant increase in absorptance in the near-ultraviolet region. This is shown in Table 6-2 in which aluminum deposited on glass (at high rate) shows a 15% increase in solar absorptance when the film thickness is varied from 505 to 4250 Å. For essentially the same conditions, except using polished aluminum alloy substrate (Table 6-3), there is a 120% increase in solar absorptance. Emittances remain

Table 6-1

EMITTANCE AND ABSORPTANCE DEPENDENCE
ON SUBSTRATE/SURFACE QUALITY

(Aluminum Deposited on Substrates Simultaneously;
No Dielectric Overcoat)

Substrate	Condition	Absorptance α_s		Emittance ϵ_L	
		Before Aluminum Deposition	After Aluminum Deposition	Before Aluminum Deposition	After Aluminum Deposition
Aluminum Alloy	Mill Finish	0.364	0.109	0.04	0.03
Aluminum Alloy	Polished	0.150	0.091	0.03	0.03
Stainless Steel	Mill Finish	0.364	0.086	0.10	0.04
Glass	As Drawn	–	0.080	–	0.04

Table 6-2

EFFECT OF FILM THICKNESS ON ABSORPTANCE
AND EMITTANCE OF ALUMINUM
ON GLASS SUBSTRATES

(Average Deposition Rate: 370 Å/sec)

Absorptance α_s	Emittance ϵ_L	Film Thickness (Å)
0.081	0.03	505
0.086	0.03	765
0.082	0.03	922
0.082	0.04	1475
0.092	0.03	2285
0.090	0.04	2642
0.091	0.04	3693
0.095	0.04	4250

approximately constant in both cases for the full range of film thickness. Stainless steel (bright finish) shows a corresponding 30% increase in α_s (Table 6-4).

Cleanliness of system and substrate, and purity of evaporant material are all important in achieving high-purity depositions. There is little reason to use six "nines" purity source material if the system is contaminated from many evaporations or if the source becomes contaminated from reevaporations of previously evaporated higher vapor pressure source material. It is not practical to completely shield the evaporation chamber so that evaporant impinges only on substrate. It is also not practical to thoroughly clean the source and chamber after each evaporation. The reasonable solution is to minimize the contamination and evaporate at high speeds after outgassing the source with the main shutter closed.

Source materials were high purity and usually vacuum melted. Little outgassing of source material was evident. In a typical system operation, the clean system pressure would start in the low 10^{-8} torr pressure range and rise to approximately 10^{-6} torr during high power inputs for rapid evaporations.

After approximately 10 to 20 evaporations, depending upon materials evaporated, the initial system pressure would be near 10^{-7} torr before source heating and would rise to near 10^{-6} torr during evaporation, again dependent upon the materials used. When pressures during evaporation approached high 10^{-5} torr, the system was completely disassembled and cleaned.

6.2.3 Kinetic Deposition Parameters

The kinetic deposition parameters are:

- Deposition rate
- Source temperature
- Substrate temperature
- Velocity
- Alloying
- Diffusion

Table 6-3

EFFECT OF FILM THICKNESS ON ABSORPTANCE AND EMITTANCE OF ALUMINUM ON POLISHED ALUMINUM ALLOY SUBSTRATE

(Average Deposition Rate: 550 Å/sec)

Absorptance α_s	Emittance ϵ_L	Film Thickness (Å)
0.079	0.03	537
0.079	0.03	658
0.086	0.03	908
0.082	0.03	1013
0.090	0.03	1461
0.086	0.03	1650
0.112	0.03	2000
0.109	0.03	2495
0.179	0.04	4753

Table 6-4

EFFECT OF FILM THICKNESS ON ABSORPTANCE AND EMITTANCE OF ALUMINUM ON STAINLESS STEEL SUBSTRATES

(Average Deposition Rate: 400 Å/sec)

Absorptance α_s	Emittance ϵ_L	Film Thickness (Å)
0.083	0.04	350
0.083	0.04	535
0.084	0.04	772
0.086	0.04	825
0.119[a]	0.04	1120
0.109	0.04	1831
0.095	0.04	2560
0.109	0.04	3235

(a) Rate: 207 Å/sec.

The dominant factor is deposition rate. Low rates of deposition result in physical adsorption of residual gases as well as chemisorption depending on evaporant. Of great importance is the necessity of creating large numbers of nucleation sites and of filling the spaces laterally before significant agglomeration can occur. Tendency to agglomerate is dependent upon substrate and film surface mobility of the evaporant material, presence of adsorbed gas, and substrate characteristics as previously discussed.

The effect of deposition rate of aluminum upon solar absorptance (glass substrate) is shown in Table 6-5. Opaque films of minimum thickness, to isolate agglomeration effects due to thickness, were deposited at rates from 10 to 1000 Å/sec. The results show a minimum deposition rate to be of the order of 200 Å/sec. No gain is shown for rates in excess of 800 Å/sec.

It should be noted that these results apply only to this system with an amorphous substrate. There is a tradeoff of rate and thickness for constant absorptance. For a polycrystalline surface, a higher rate of evaporation (of the order of 400 to 600 Å/sec) would be necessary to obtain low solar absorptance.

Deposition rate effects upon absorptance are not as critical with silver and gold on glass substrates (Tables 6-6 and 6-7).

Source temperature and impingement velocity are related. In general, source temperature is maintained as low as possible, consistent with desired deposition rate. This is particularly important with dielectrics, in which case evaporation power density is kept low to minimize dissociation. Dielectric evaporation rates were typically 10 to 30 Å/sec.

Substrate temperatures were between room temperature and 310°K. At this temperature, alloying and diffusion are insignificant for the materials deposited. However, there is a possibility that recrystallization may occur with silver.

Table 6-5

EFFECT OF DEPOSITION RATE ON ABSORPTANCE AND EMITTANCE OF ALUMINUM ON GLASS SUBSTRATES

(Aluminum Thickness: 700−900 Å)

Absorptance α_s	Emittance ϵ_L	Deposition Rate (Å/sec)
0.096	0.05	10
0.092	0.05	21
0.084	0.05	93
0.084	0.05	129
0.082	0.05	175
0.084	0.05	275
0.083	0.04	420
0.081	0.04	805
0.081	0.04	1000

Table 6-6

EFFECT OF DEPOSITION RATE ON ABSORPTANCE AND EMITTANCE OF SILVER ON GLASS SUBSTRATES

(Silver Thickness: 2000 Å)

Absorptance α_s	Emittance ϵ_L	Deposition Rate (Å/sec)
0.043	0.03	20
0.042	0.03	43
0.041	0.03	104
0.041	0.03	170
0.040	0.03	570
0.040	0.03	725

Table 6-7

EFFECT OF DEPOSITION RATE ON ABSORPTANCE AND EMITTANCE OF GOLD ON GLASS SUBSTRATES

(Gold Thickness: 2140−2600 Å)

Absorptance α_s	Emittance ϵ_L	Rate (Å/sec)
0.178	0.03	60
0.176	0.03	93
0.177	0.03	168
0.180	0.03	260

The evaporation of silver by electron bombardment presented problems that do not normally occur with conventional resistance-heated silver sources. For processing and equipment simplicity, it was decided to evaporate silver and gold by electron beam heating instead of the simple resistance heating method. In the case of silver, this method proved to be very troublesome. Silver, having very high mobility, condenses on the electron beam gun structure and crucible shields. After a number of evaporations, some of the silver presumably forms extensive oxide layers. This oxide appears not only to be unstable, but also to have relatively high vapor pressure and, apparently, high mobility (Refs. 12 and 13). To minimize this effect, the electron beam gun was modified with a water-cooled anode (as discussed in Section 4). Also, the silver was evaporated from a shallow tungsten pan of small capacity, as opposed to evaporation from a large-capacity ceramic crucible.

An effect noted was the condensation of straw to red-brown colored films. These contamination films caused high absorptance of the silver surface. These deposits occurred on the other side of the evaporant condensing side, which was completely shielded from the source. This could not be explained by scattering, since pressure was in the low 10^{-6} torr range. A red-brown film would form when operating with the substrate shutters fully open followed by sequential closing of the shutters to obtain increasing film thickness at each substrate while maintaining deposition parameters constant. The closed substrate shutters completely obscured the source from the substrate surface. This effect did not appear if the substrate shutters were left open. It was assumed that this contamination film was a silver oxide, possibly Ag_2O.

It is noted that silver has an oxygen atmospheric solubility of 20 times its own volume near its melting point (1246°K), whereas it has a solubility of only 0.56 its volume with a temperature drop of 50°K. This magnitude of change, however, would not be expected at low pressures. There are indications of a readily reversible reaction of silver oxide to silver with small changes of pressure and temperature.

6.3 OPTICAL CHARACTERISTICS

These are established by the material optical properties and the film morphology, which in turn is controlled by the parameters given in subsection 6.2.1. The changes in optical characteristics, solar absorptance α_s, and emittance ϵ_L as a function of the thickness of the dielectric overlay on a reflective metal surface, are shown in Figs. 6-1 through 6-6.

The importance of preventing source contamination from material of source crucible is shown. Evaporation techniques were modified when inconsistent results showed that alumina crucible liners (in contact with water-cooled copper surfaces) were contaminating the source material. This was a significant factor with dielectric materials. Dielectric materials were evaporated from fully loaded water-cooled copper crucibles.

The evaporation of silica presented no problems. The material was in the form of random-size chips approximately 1/16 in. thick and varying from 1/8 in. to 1/2 in., generally square in shape. The evaporant sublimated preferentially from the sharp broken edges of a large number of exposed, randomly oriented pieces. The water-cooled copper crucible cavity was filled to overflowing.

The evaporation of alumina presented no serious problems. The technique in positioning the electron beam impingement area is important in obtaining uniform deposition. The source material was large chips from a sapphire boule. If the pieces were long relative to their thickness, there was a tendency for the beam to undercut the piece on the emitter side. The obscuring or shading of the evaporation vapor from large areas of the substrate holder by the overhang of the top of the evaporant source material resulted in very nonuniform film thickness from substrate to substrate and over the substrate area. This can be observed by interference colors. The solution to this problem was to impinge the electron beam onto the top of a hummock-shaped piece of the boule. The area of impingment

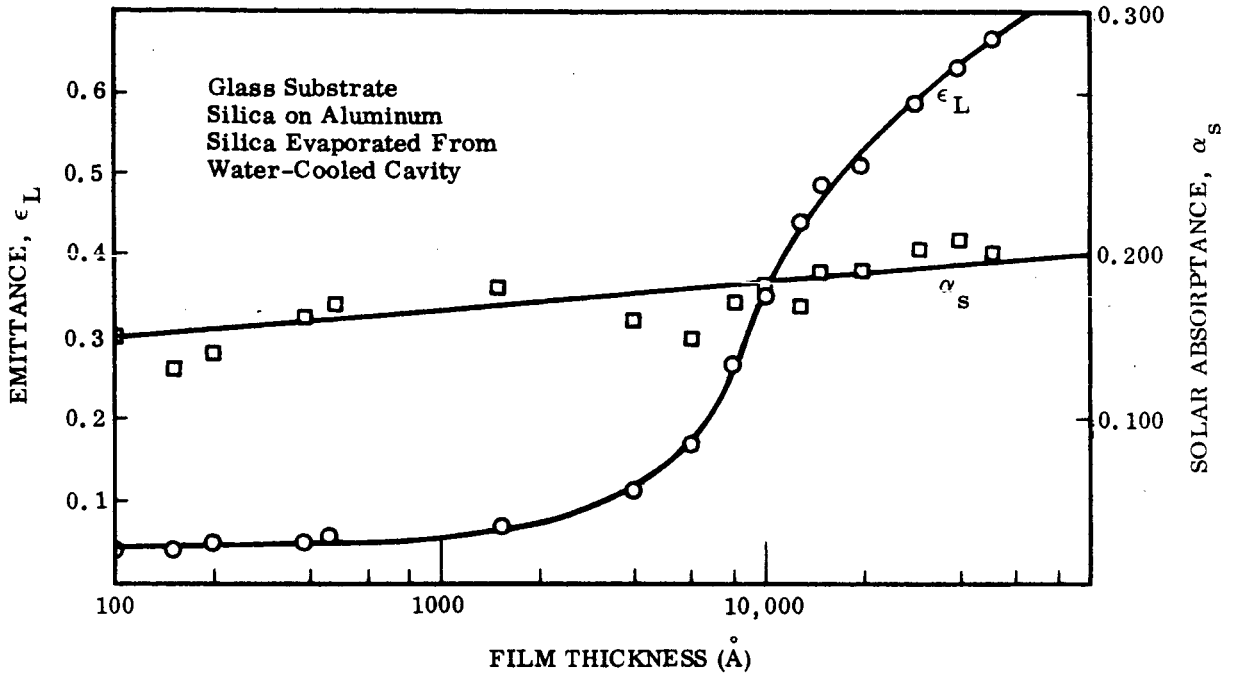

Fig. 6-1. Silica-Aluminum-Glass System – Solar Absorptance α_s and Emittance ϵ_L Versus Silica Film Thickness (No Crucible)

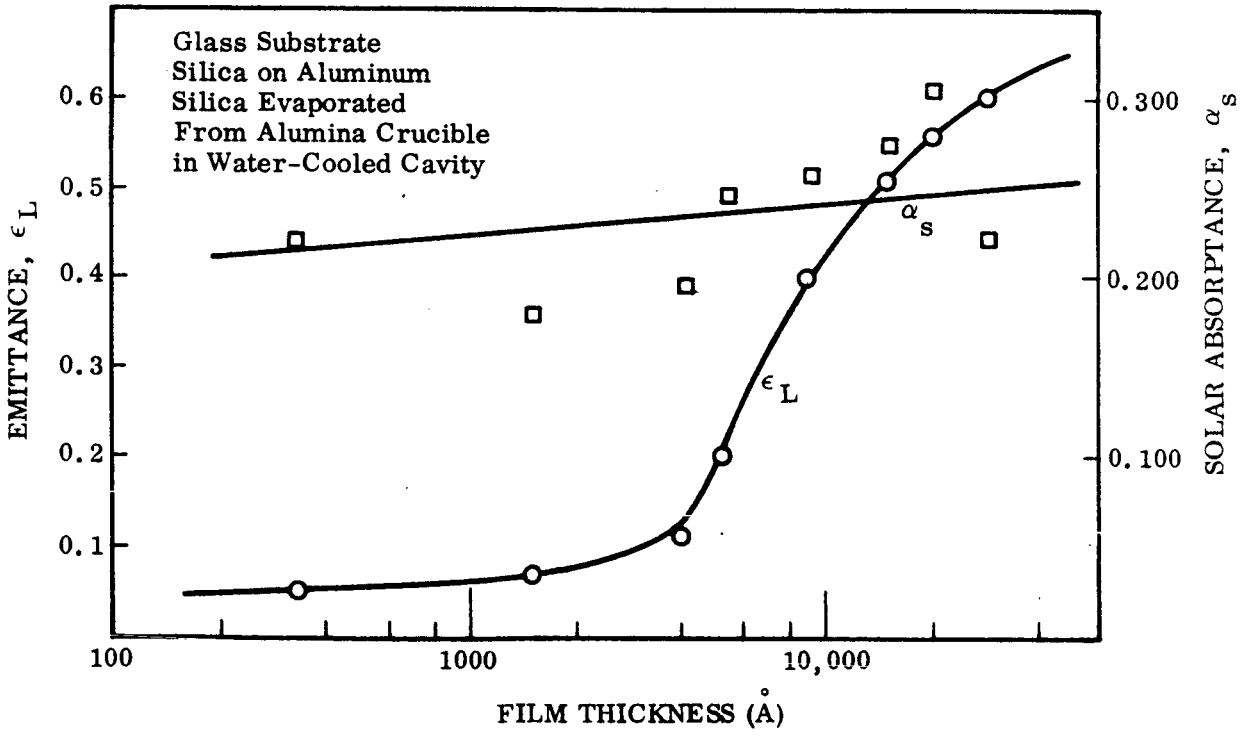

Fig. 6-2 Silica-Aluminum-Glass System – Solar Absorptance α_s and Emittance ϵ_L Versus Silica Film Thickness (Alumina Crucible)

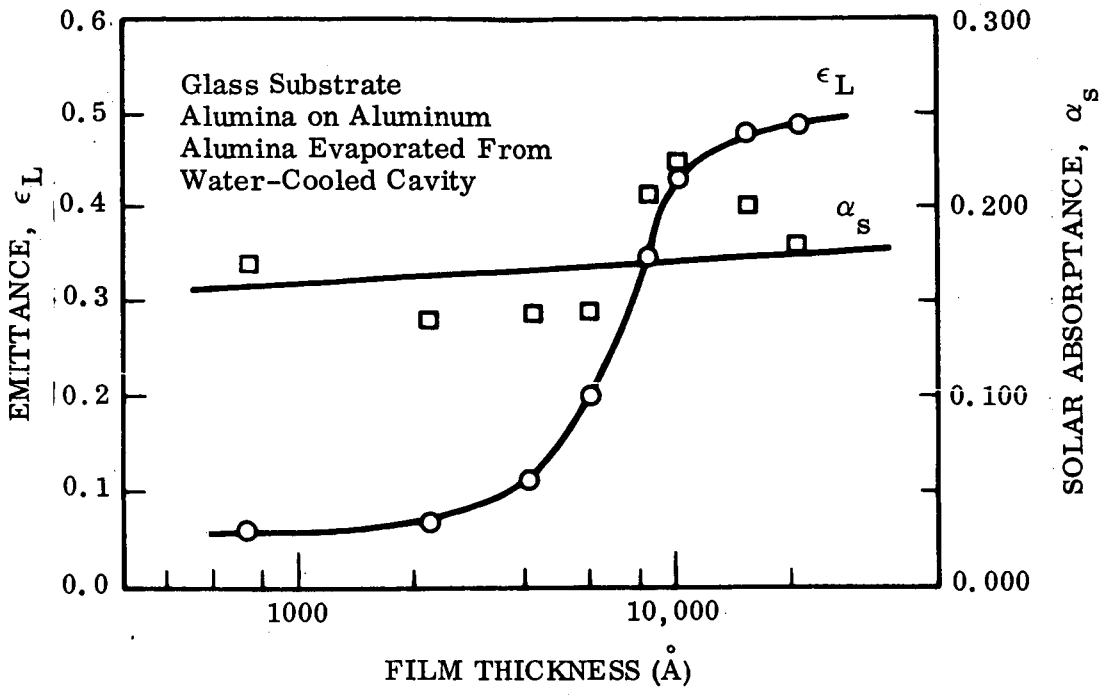

Fig. 6-3 Alumina-Aluminum-Glass System – Solar Absorptance α_s and Emittance ϵ_L Versus Alumina Film Thickness (No Crucible)

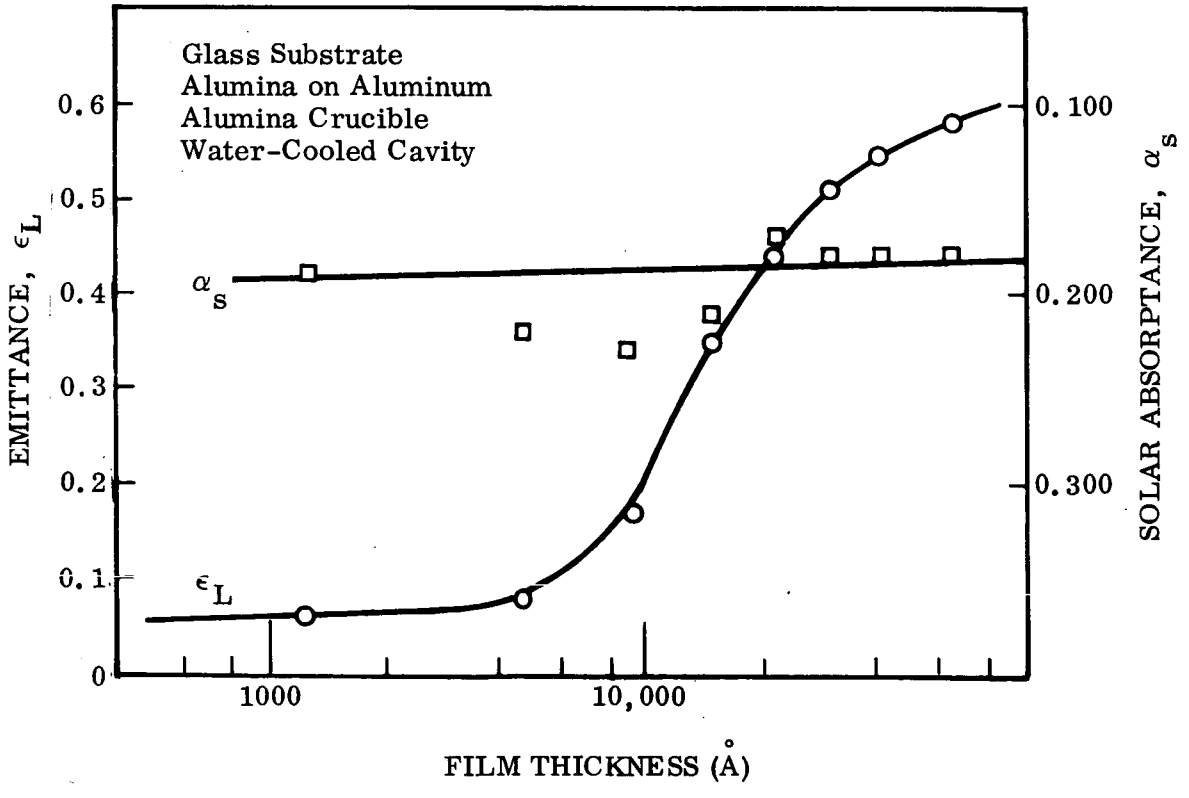

Fig. 6-4 Alumina-Aluminum-Glass System – Solar Absorptance α_s and Emittance ϵ_L Versus Alumina Film Thickness (Alumina Crucible)

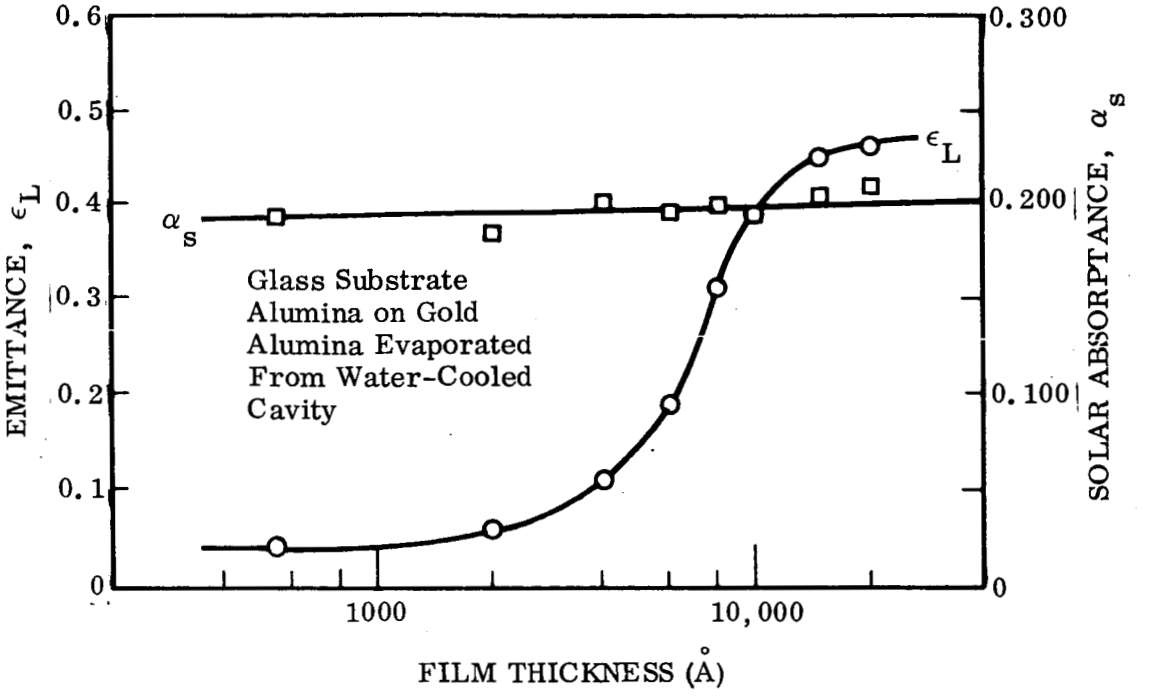

Fig. 6-5 Alumina-Gold-Glass System – Solar Absorptance α_s and Emittance ϵ_L Versus Alumina Film Thickness

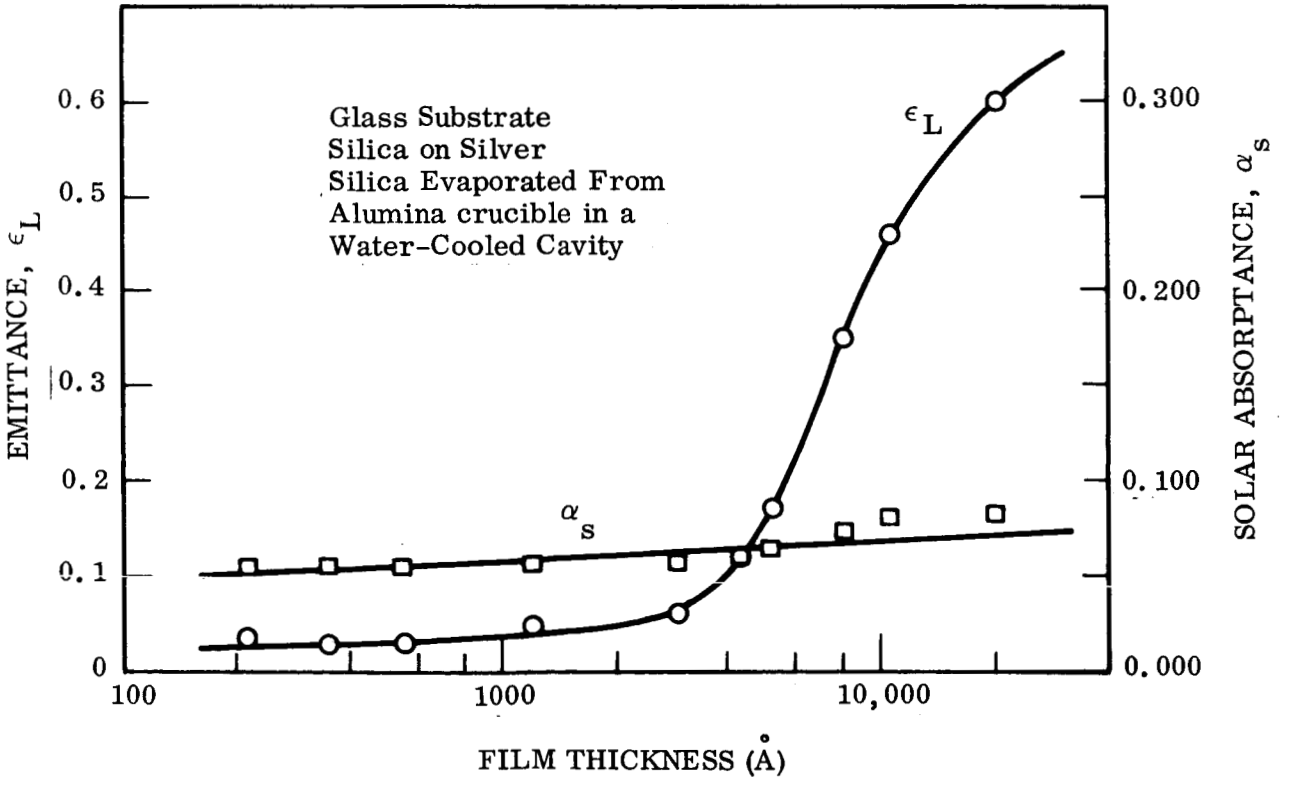

Fig. 6-6 Silica-Silver-Glass System – Solar Absorptance α_s and Emittance ϵ_L Versus Silica Film Thickness (Alumina Crucible)

appears as a swirling vapor. A small surface area appeared to be in the liquid phase. The liquid phase did not extend over the impingement area much more at high evaporation rates than at low rates.

In the case of aluminum, it was difficult to evaporate at rates higher than 150 Å/sec when aluminum was in contact with the water-cooled copper crucible. Five kilowatts electron beam power were used. This method was undesirable because of alloying action occurring between the aluminum and copper.

The crucible finally used for high aluminum evaporation rates, which results in no source contamination, consisted of a multi-strand tungsten helix placed on a tungsten pan with a shallow depression. Aluminum pellets were placed in the helix. During evaporation, the liquid aluminum was supported in the helix in the form of a ball due to surface tension. The tungsten pan, supported on its edges by a water-cooled copper surface, remained at a lower temperature than the helix. The pan acted as an aluminum reservoir as liquid aluminum wicked up the helix. The net result is similar to conventional aluminum evaporation from a resistance-heated tungsten helix, with the advantage that the tungsten helix was at a lower temperature than the evaporating aluminum ball. This further minimized the possibility of tungsten evaporation, which is usually a negligible problem when evaporation is made from a resistance-heated tungsten helix. Rates in excess of 1000 Å/sec were accomplished with less than 3 kW. Silver and gold were evaporated from tungsten pans without the helix.

It should be noted that the comments made regarding alumina crucibles apply even more so with "composite" crucibles containing titanium diboride and boron nitride. Source contamination was copious using these crucibles with electron beam heating. This does not preclude their use as resistance-heated crucibles. The use of "composite" crucibles even in this case would have to be done with caution if consistent and quality optical surfaces are sought. The emittance of the dielectric overlay is very sensitive to dielectric source material contamination. Similarly, solar absorptance of the metal reflective surface is increased with a contaminated source.

The curves of emittance ϵ_L in Figs. 6-1 through 6-6 show linear increase of emittance with increasing dielectric thickness from 100 to approximately 2000 Å of dielectric thickness. The increase is then exponential until a leveling-off occurs as bulk emittance values are approached.

Representative spectrophotometer traces are shown of various coating systems investigated in Figs. 6-7 through 6-12. Some variations in absorptance occur in the near-ultraviolet to visible range due to interference effects of the 1000 Å dielectric thicknesses.

6.4 ULTRAVIOLET ENVIRONMENTAL TEST RESULTS AND OPTICAL MEASUREMENTS

A screening test was conducted with all the combinations of substrates, metals, and dielectrics to be investigated. The results of the screening are shown in Table 6-8.

In general, little optical degradation occurred with the exception of the coating system of silica on gold on aluminum alloy substrate. This system showed catastrophic failure. There was separation of the gold from the aluminum alloy substrate, as well as failure of the silica gold interface. Interestingly, this did not occur with glass or stainless steel substrates, nor was there any degradation when alumina was used as the dielectric instead of silica. Apparently the failure was due to thermal mismatch of the substrate and coating, although a detailed study of the failure phenomenon was beyond the scope of the program.

From the results of these screening tests and from consideration of material end use and desired optical characteristics, three coating systems were selected to meet the program requirements. The systems selected for more extensive environmental testing were:

System No.	Optical Characteristics	Coating System
I	$\alpha_s/\epsilon < 0.1$	OSR (Silver-fused silica second surface mirror)
II	$\alpha_s/\epsilon \approx 1.0$ $\alpha_s < 0.1$	Silica on silver on polished aluminum alloy substrate
III	Minimum ϵ	Alumina on silver on mill-finish aluminum alloy substrate

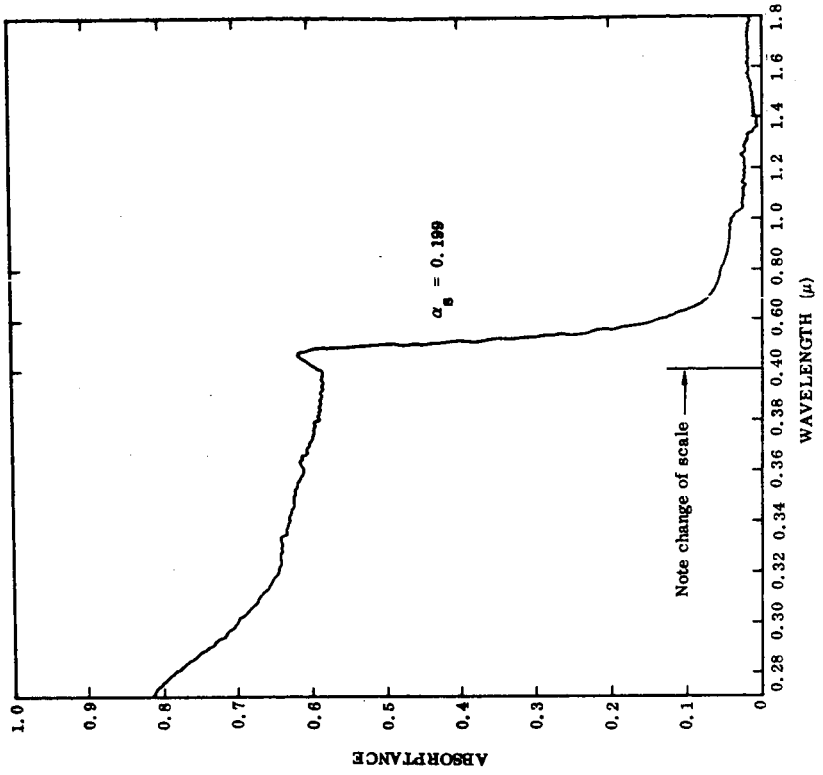

Fig. 6-8 Absorptance of 1000 Å Silica on 1730 Å Gold (Polished Aluminum Alloy Substrate)

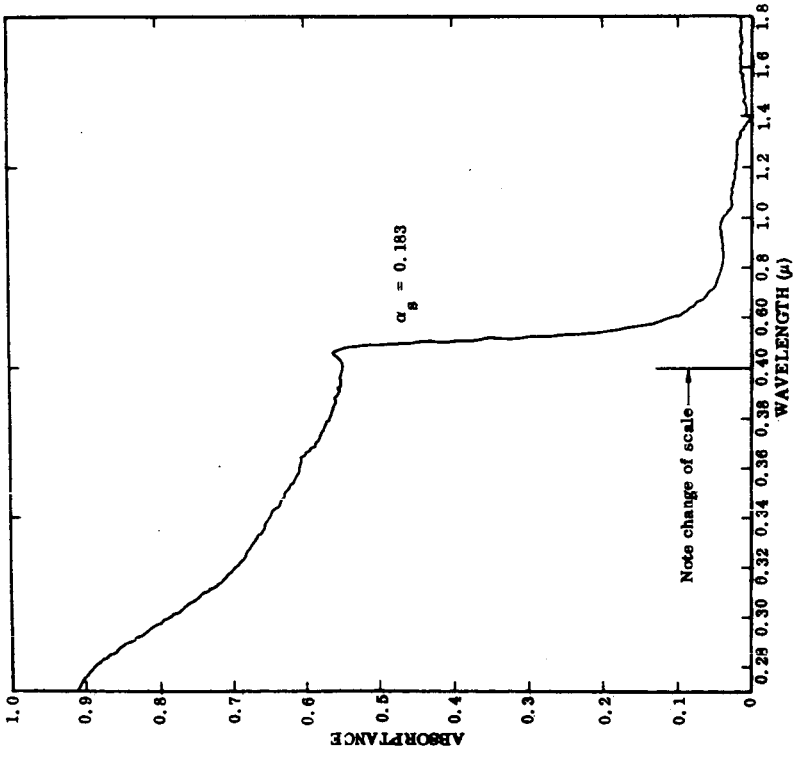

Fig. 6-7 Absorptance of 985 Å Alumina on 730 Å Gold (Polished Aluminum Alloy Substrate)

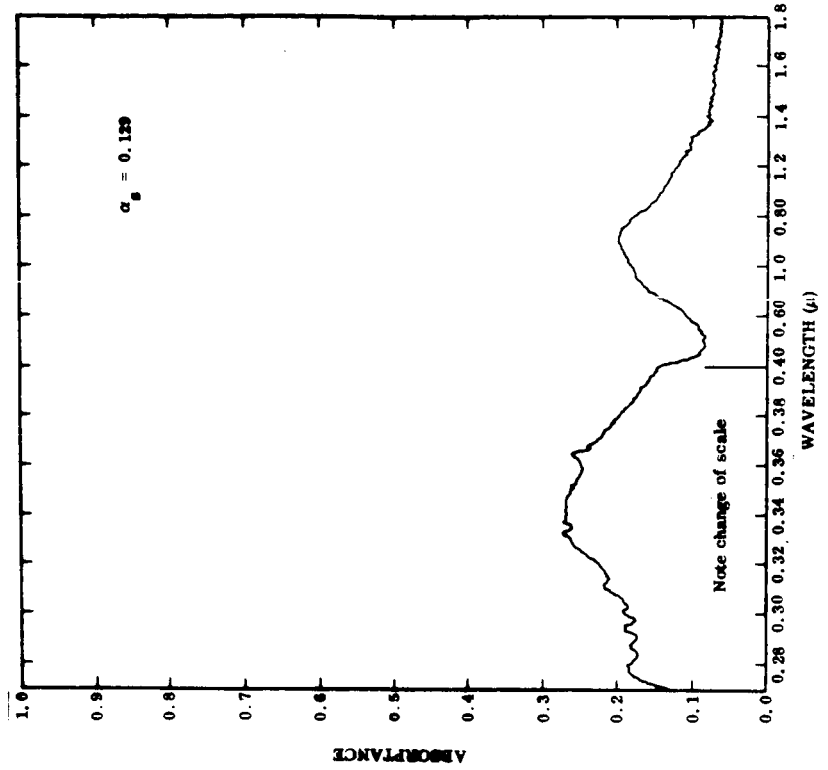

Fig. 6-10 Absorptance of 1030 Å Alumina on 740 Å Aluminum (Polished Aluminum Alloy Substrate)

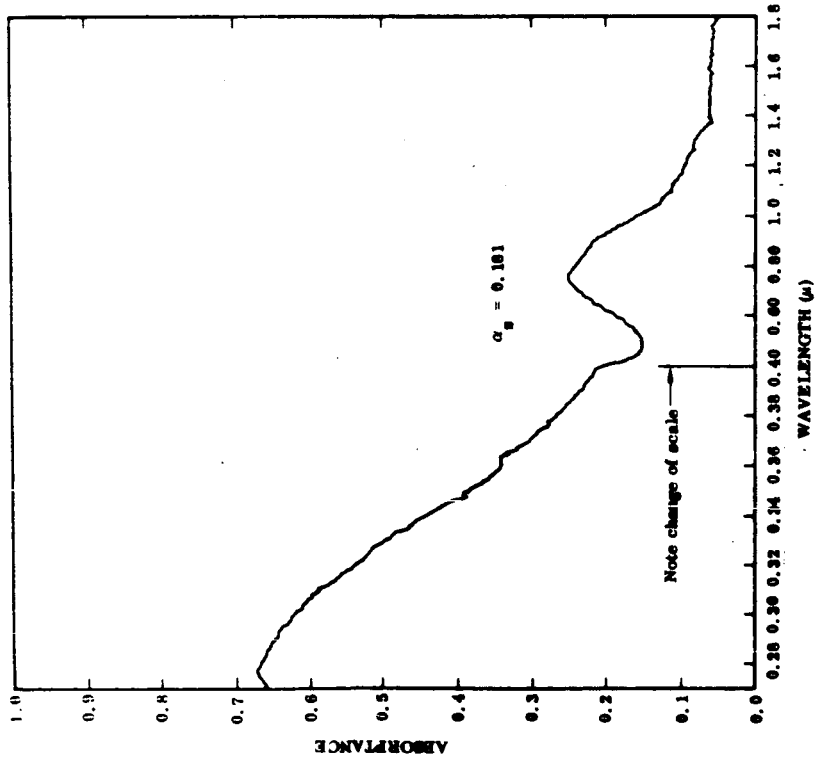

Fig. 6-9 Absorptance of 1010 Å Silica on 1040 Å Aluminum (Polished Aluminum Alloy Substrate)

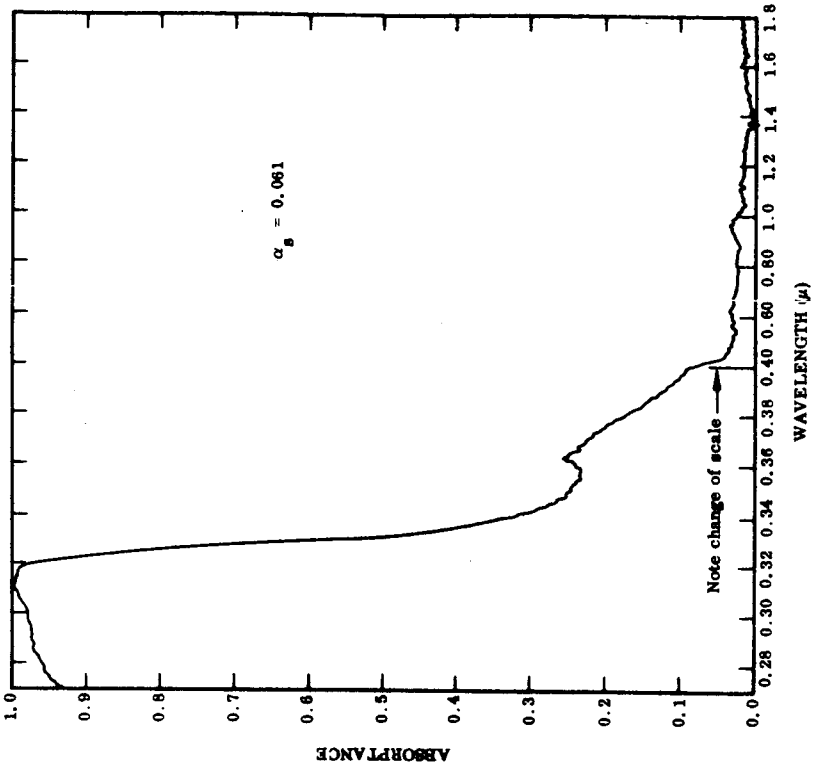

Fig. 6-12 Absorptance of 1010 Å Silica on 1450 Å Silver (Polished Aluminum Alloy Substrate)

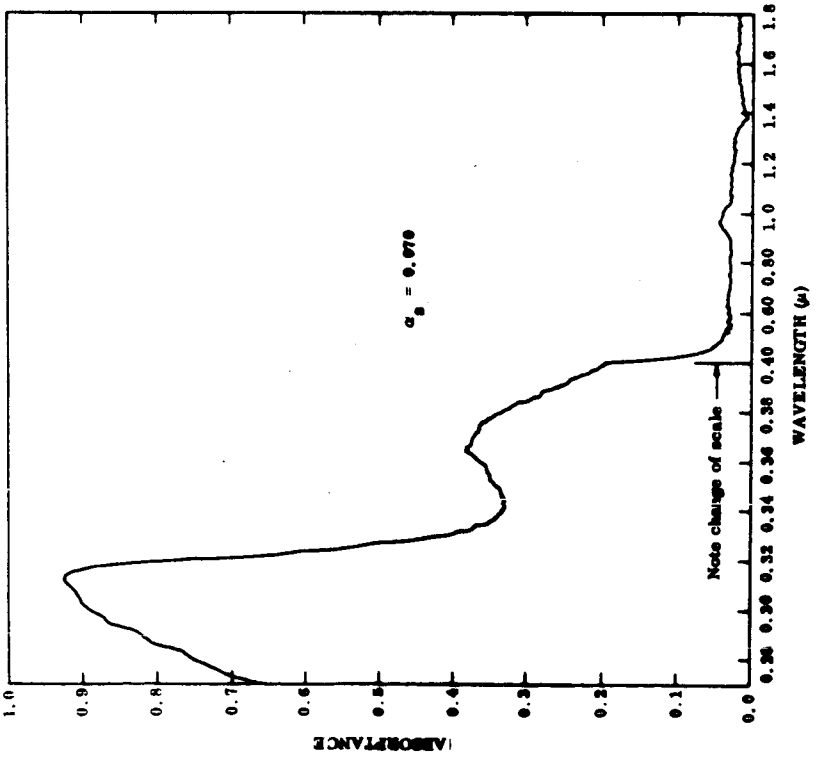

Fig. 6-11 Absorptance of 960 Å Alumina on 970 Å Silver (Polished Aluminum Alloy Substrate)

Table 6-8

RESULTS OF SCREENING TEST
250 EQUIVALENT SUN-HOURS OF ULTRAVIOLET AT 533°K
10 THERMAL CYCLES

Substrate	Metal[c]	Overcoat 1000 Å	Absorptance[a]		Emittance[b]	
			Initial	Final	Initial	Final
Glass	Gold	Silica	0.187	0.178	0.03	0.045
	Silver		0.051	0.051	0.04	0.035
	Aluminum		0.126	0.122	0.07	0.06
	Gold	Alumina	0.181	0.180	0.03	0.045
	Silver		0.056	0.060	0.04	0.04
	Aluminum		0.139	0.128	0.06	0.06
Polished Aluminum Alloy	Gold	Silica	0.199	Sample Failure	0.03	Sample Failure
	Silver		0.061	0.061	0.04	0.03
	Aluminum		0.181	0.185	0.06	0.05
	Gold	Alumina	0.183	0.186	0.03	0.035
	Silver		0.070	0.074	0.04	0.03
	Aluminum		0.129	0.134	0.07	0.05
Mill Finish Aluminum Alloy	Gold	Silica	0.206	Sample Failure	0.03	Sample Failure
	Silver		0.085	0.080	0.04	0.035
	Aluminum		0.184	0.177	0.06	0.04
	Gold	Alumina	0.215	0.217	0.04	0.04
	Silver		0.105	0.101	0.04	0.04
	Aluminum		0.163	0.149	0.07	0.06
Stainless Steel	Gold	Silica	0.202	0.202	0.02	0.04
	Silver		0.071	0.061	0.04	0.035
	Aluminum		0.164	0.169	0.06	0.04
	Gold	Alumina	0.199	0.204	0.03	0.035
	Silver		0.076	0.077	0.04	0.03
	Aluminum		0.141	0.135	0.07	0.04
OSR	TP-060		0.045	0.042	0.76	0.76

(a) Solar absorptance values valid within ± 0.005.
(b) Emittance values from Lion emissometer valid within ± 0.01.
(c) Nominal thickness of 2000 Å.

The environmental testing was performed for 2000 ESH with substrates at 294°K and at 533°K. The results of these tests are shown in Tables 6-9 and 6-10.

System I showed no change in optical characteristics as a result of any of the environmental tests. System II showed an increase in solar absorptance from 0.072 to 0.076 when the substrates were at 533°K and an increase from 0.063 to 0.078 with the substrates at 294°K. Emittances remained constant. System III showed an increase in solar absorptance from 0.074 to 0.125 with the substrates at 533°K and an increase from 0.074 to 0.076 with the substrates at 294°K. Emittances remained constant.

Changes in absorptance over the range of 0.275 to 1.8 μ as a result of environmental testing are shown in the spectrophotometer curves, Figs. 6-13 through 6-16. Figure 6-17 shows OSR absorptance before ultraviolet exposure which is the same after exposure. Table 6-11 shows absorptance and emittance of the three selected coating systems. The emittances measured were ϵ_L (Lion Optical Surface Comparator), ϵ_N (normal), and ϵ_H (total) hemispherical) at various temperatures. Table 6-12 shows the calculated emittance for various temperatures from 294° to 555° K for each of the three selected systems.

Table 6-9

EFFECT OF ULTRAVIOLET IRRADIATION ON OSR AND SILICA/ALUMINA-ALUMINUM ALLOY SYSTEMS – 2000 SUN-HOURS OF ULTRAVIOLET AT 294°K

Substrate	Metal Film (c)	Dielectric Overcoat		Absorptance(a) α_s		Emittance(b) ϵ_L	
		Thickness (Å)	Material	Initial	Final	Initial	Final
OSR	Silver	–	–	0.048	0.047	0.74	0.74
Polished Aluminum Alloy	Silver	1000	Silica	0.084	0.108	0.03	0.03
	Silver	2000	Silica	0.067	0.077	0.04	0.04
	Silver	3000	Silica	0.063	0.078	0.07	0.06
Mill-Finish Aluminum Alloy	Silver	1000	Alumina	0.074	0.076	0.03	0.03

(a) Solar absorptance values valid within ± 0.005.
(b) Emittance values valid within ± 0.01.
(c) Nominal thickness of 2000 Å.

Table 6-10

EFFECT OF ULTRAVIOLET IRRADIATION ON OSR AND SILICA/ALUMINA-ALUMINUM ALLOY SYSTEMS – 2000 SUN-HOURS OF ULTRAVIOLET AT 533°K

Substrate	Metal Film (c)	Dielectric Overcoat		Absorptance(a) α_s		Emittance(b) ϵ_L	
		Thickness (Å)	Material	Initial	Final	Initial	Final
OSR	Silver	–	–	0.052	0.049	0.74	0.74
Polished Aluminum Alloy	Silver	1010	Silica	0.087	0.109	0.03	0.03
	Silver	2000	Silica	0.063	0.068	0.04	0.04
	Silver	3000	Silica	0.072	0.076	0.07	0.07
Mill-Finish Aluminum Alloy	Silver	1000	Alumina	0.074	0.125	0.03	0.04

(a) Solar absorptance values valid within ± 0.005.
(b) Emittance values valid within ± 0.01.
(c) Nominal thickness of 2000 Å.

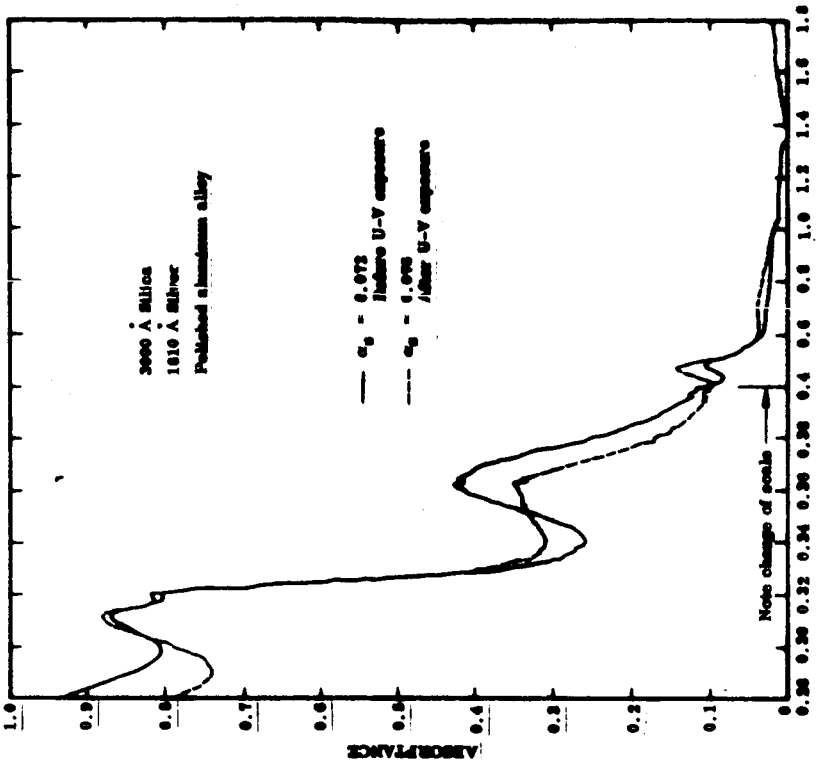

Fig. 6-13 Effect of UV Irradiation on Absorptance; Silica-Silver-Aluminum Alloy System; Substrate at 294°K – 2000 ESH

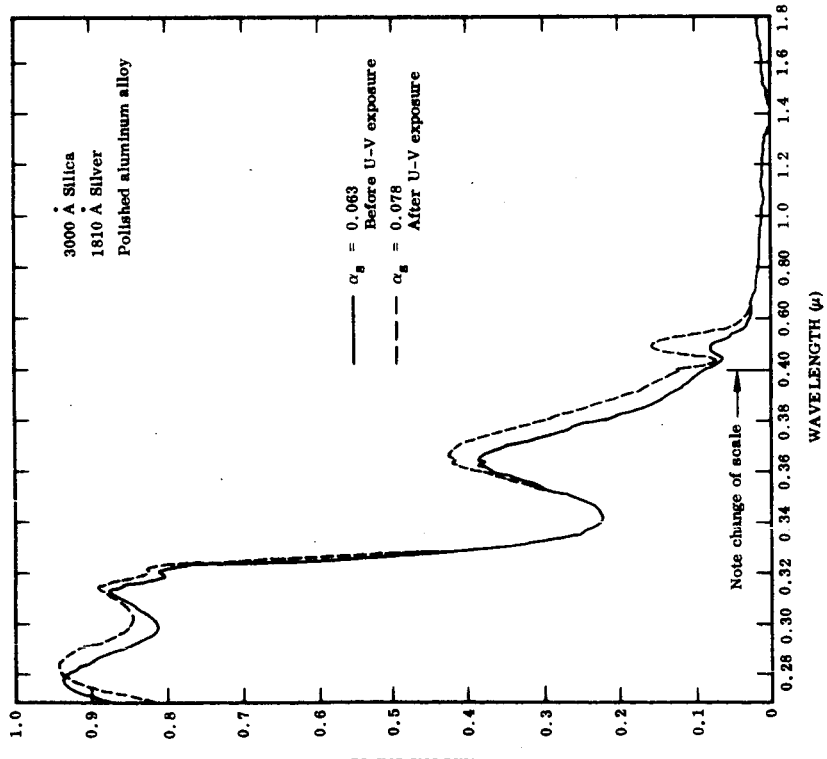

Fig. 6-14 Effect of UV Irradiation on Absorptance; Silica-Silver-Aluminum Alloy System; Substrate at 533°K – 2000 ESH

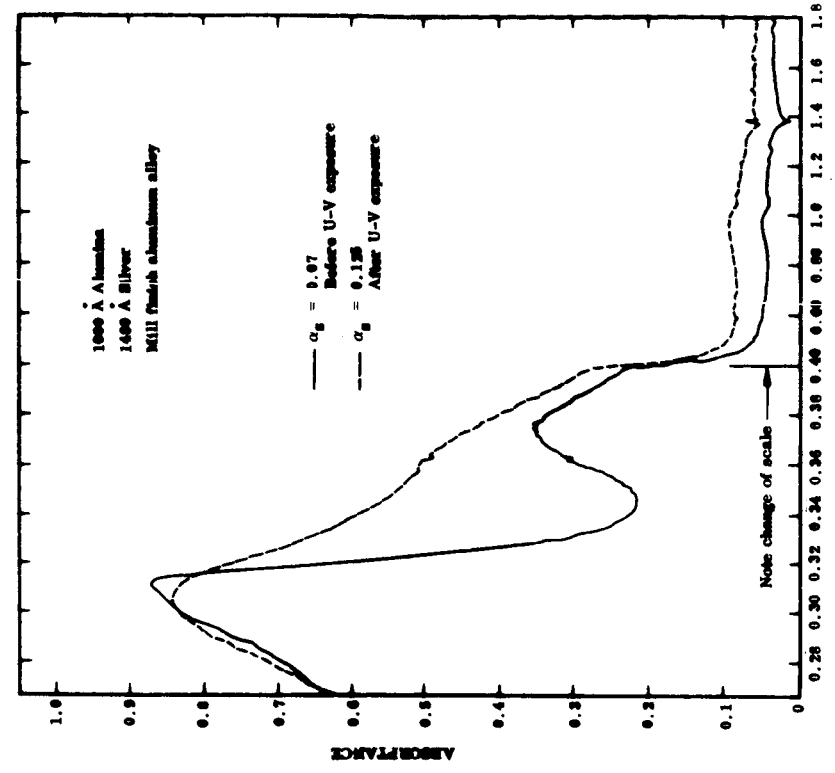

Fig. 6-16 Effect of UV Irradiation on Absorptance; Alumina-Silver-Aluminum Alloy System; Substrate at 533°K – 2000 ESH

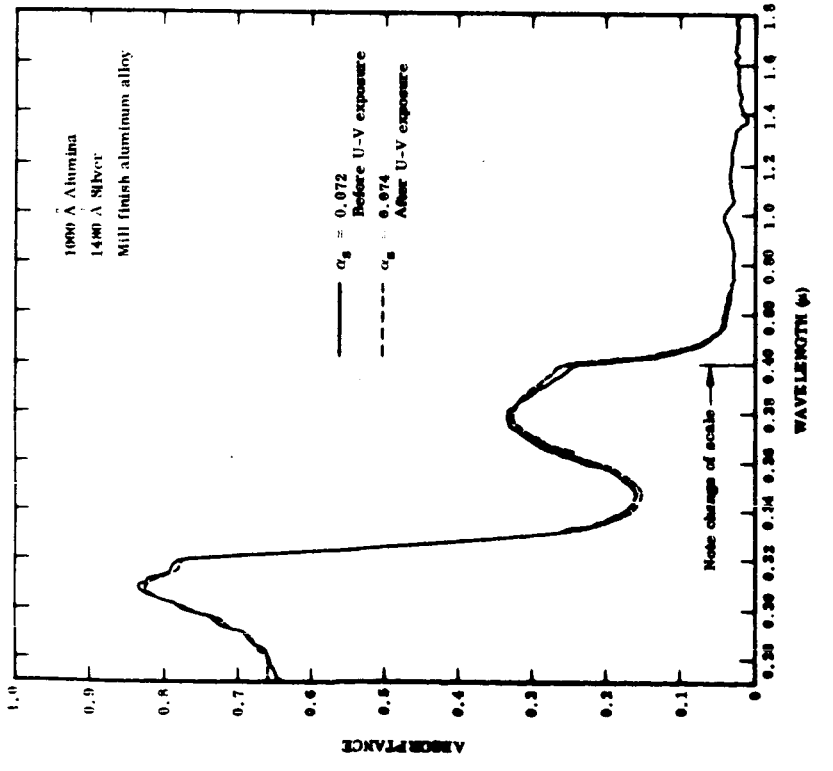

Fig. 6-15 Effect of UV Irradiation on Absorptance; Alumina-Silver-Aluminum Alloy System; Substrate at 294°K – 2000 ESH

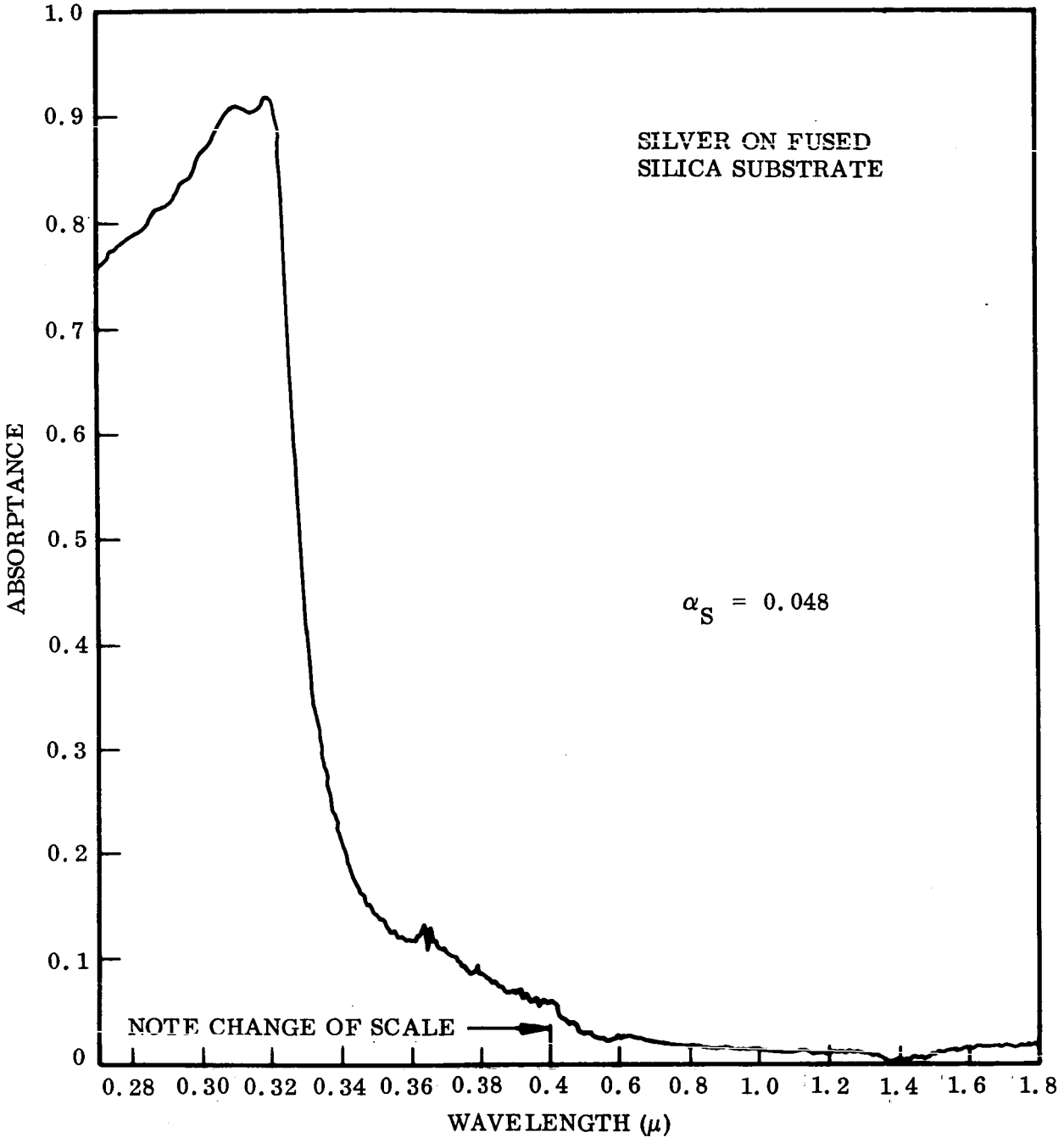

Fig. 6-17 Absorptance of OSR

Table 6-11

OPTICAL CHARACTERISTICS OF SELECTED COATING SYSTEMS

Coating System	Absorptance α_s	Emittance				
		ϵ_L	ϵ_N 300°K 2 – 25μ	ϵ_H		
				Low Temp.	Intermediate Temp.	High Temp.
I. OSR ($\alpha_s/\epsilon < 0.1$)	0.048	0.74	0.75	0.744 (144°K)	0.81 (255°K)	0.790 (366°K)
II. Silica-Silver-Aluminum Alloy System $\alpha_s/\epsilon \approx 1.0$ $\alpha_s < 0.1$ Polished Substrate	0.063	0.07	0.034	0.061 (110°K)	0.085 (257°K)	0.101 (367°K)
III. Alumina-Silver-Aluminum Alloy System Minimum ϵ Mill-Finish Substrate	0.072	0.03	0.014	0.041 (120°K)	0.057 (264°K)	0.049 (402°K)

Table 6-12

CALCULATED EMITTANCE

Coating System	Temperature (°K)				
	294	333	389	444	555
I. OSR ($\alpha_s/\epsilon < 0.1$)	0.75	0.77	0.79	0.77	0.73
II. Silica-Silver-Aluminum Alloy System [$\alpha_s/\epsilon \approx 1.0$, $\alpha_s < 0.1$] Polished Substrate	0.034	0.035	0.035	0.036	0.038
III. Alumina-Silver-Aluminum Alloy System Mill-Finish Substrate (Minimum ϵ)	0.014	0.014	0.014	0.014	0.015

Section 7
DISCUSSION

7.1 VAPOR-DEPOSITED FILMS

The interpretation of the optical measurements made on the various metal, dielectric, and dielectric-metal-substrate coating systems must be made with caution. The results for the specific coating systems may not be directly applicable if there are minor variations in process conditions. A variation in temper of the same aluminum alloy, a different alloy, or a variation in mill-surface finish could cause changes in absorptance but may not affect emittance.

Changes in glass composition would not affect the optical characteristics relative to the specific glass used in this investigation. An exception might be the case of a high-alkaline-content glass wherein there may be chemical attack of the metal film as a result of ion migration.

In the evaporation of metal films for low absorptance, it is essential to deposit at high rates, of the order of 500 Å/sec, in the case of aluminum; this will compensate for other process parameters that may not be optimum.

In the case of gold, it is difficult not to obtain films of good optical quality.

Silver presents some special problems. Silver films are highly sensitive; morphological changes can result from film stress or substrate heating during evaporation. Recrystallization can occur near room temperature. There is no significant increase in crystal growth unless the substrate is heated. Variations were noted in the absorptance of silver deposited on a number of aluminum alloy substrates that were deposited at the same time under the same nominal conditions. During a deposition onto eight

substrates, four substrates view the silver evaporation source only, and four view the silver source and the electron emission source. There was no significant difference in substrate temperature at different substrate positions as measured by thermocouple. It is postulated that the additional heat radiated from the electron emitter to the condensing surface was sufficient to cause film structure changes. A solution to this problem is to evaporate at lower rates to minimize substrate surface heating, since silver is not as sensitive to deposition rate as is aluminum.

The dielectric overlays presented no difficulty with the exception of the silica-gold-aluminum alloy system. The dielectric films were stable and provided excellent mechanical protection for the soft metal films.

The data obtained from a limited number of specimens subjected to elevated temperature (533° K) strongly suggest that the optical degradation of these coating systems is a result of thermal diffusion of the reflective metal film into the substrate. In addition, there may be a failure mechanism due to thermal expansion mismatch, as exemplified by the silica-gold-aluminum alloy system. The relatively minor optical degradation that did occur in the selected coating systems was evident in specimens that were ultraviolet irradiated with the substrate temperature at 533° K. Under the same test conditions, with the exception that the substrate temperature was maintained at 294° K, the degradation was insignificant.

The experimental evidence is not sufficient to fully support the hypothesis of diffusion-caused optical degradation; however, two test specimens do support this hypothesis. One specimen, with an alumina-gold-aluminum alloy coating system, was subjected to 2000 ESH at 294° K. The solar absorptance changed from 0.210 to 0.208 With the substrate at 533° K and the same test conditions, the solar absorptance increased from 0.215 to 0.507. This degradation is suggested as being a result of the high rate of intermetallic diffusion of gold.

The second test specimen, an alumina-silver-aluminum alloy coating system, showed a change in absorption (exposure with substrate at 294° K) from 0.074 to 0.076. With the

substrate at 533° K, the solar absorptance changed from 0.074 to 0.125. An identical coating system and test exposure, with the exception of the addition of 300 Å of chromium between the substrate and the reflective silver film, showed a change in solar absorptance from 0.087 to 0.095 at 294° K and from 0.091 to 0.098 at 533° K.

7.2 OPTICAL MEASUREMENTS

7.2.1 Emittance Measurements

The emittance of each candidate coating system was determined by three independent methods: (1) calorimetric measurement of total hemispherical emittance, (2) calculation of normal emittance via integration of spectral emittance in the 2 to 25-μ region, and (3) direct evaluation using the Lion Optical Surface Comparator.

The values of emittance determined calorimetrically have the most relevance to the goals of the program, since the total hemispherical emittance is the controlling factor in heat rejection by coating systems. The other methods, while possessing restricted validity, can be performed more rapidly and can thereby serve to establish qualitative trends and monitor sample-to-sample reproducibility.

The Lion Optical Surface Comparator measurements are based on the relative emittances of predetermined standards and the sample to be measured. Owing to a restricted view factor inherent in the instrument, differences between the angular distribution of emitted energy of the standards and samples lead to values of emittance intermediate between hemispherical and normal. For high-emittance materials, the recorded values approach those corresponding to near-normal emittance, whereas for low-emittance samples the values more closely approximate the total hemispherical condition.

Directional spectral reflectance properties were measured over the spectral range extending from 2 to 25 μ (Figs. 7-1, 7-2, and 7-3), from which the normal emittance

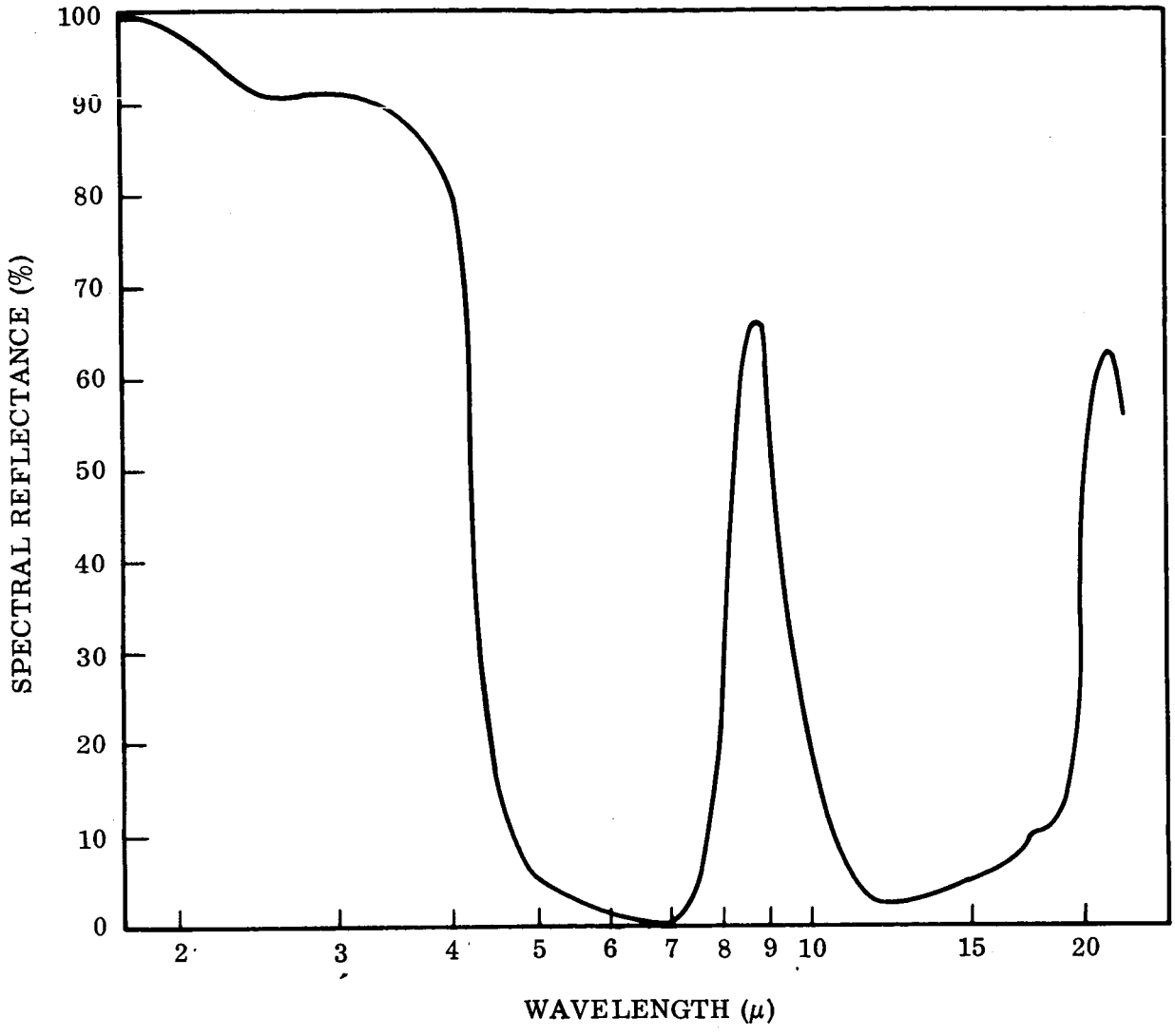

Fig. 7-1 Spectral Reflectance of OSR

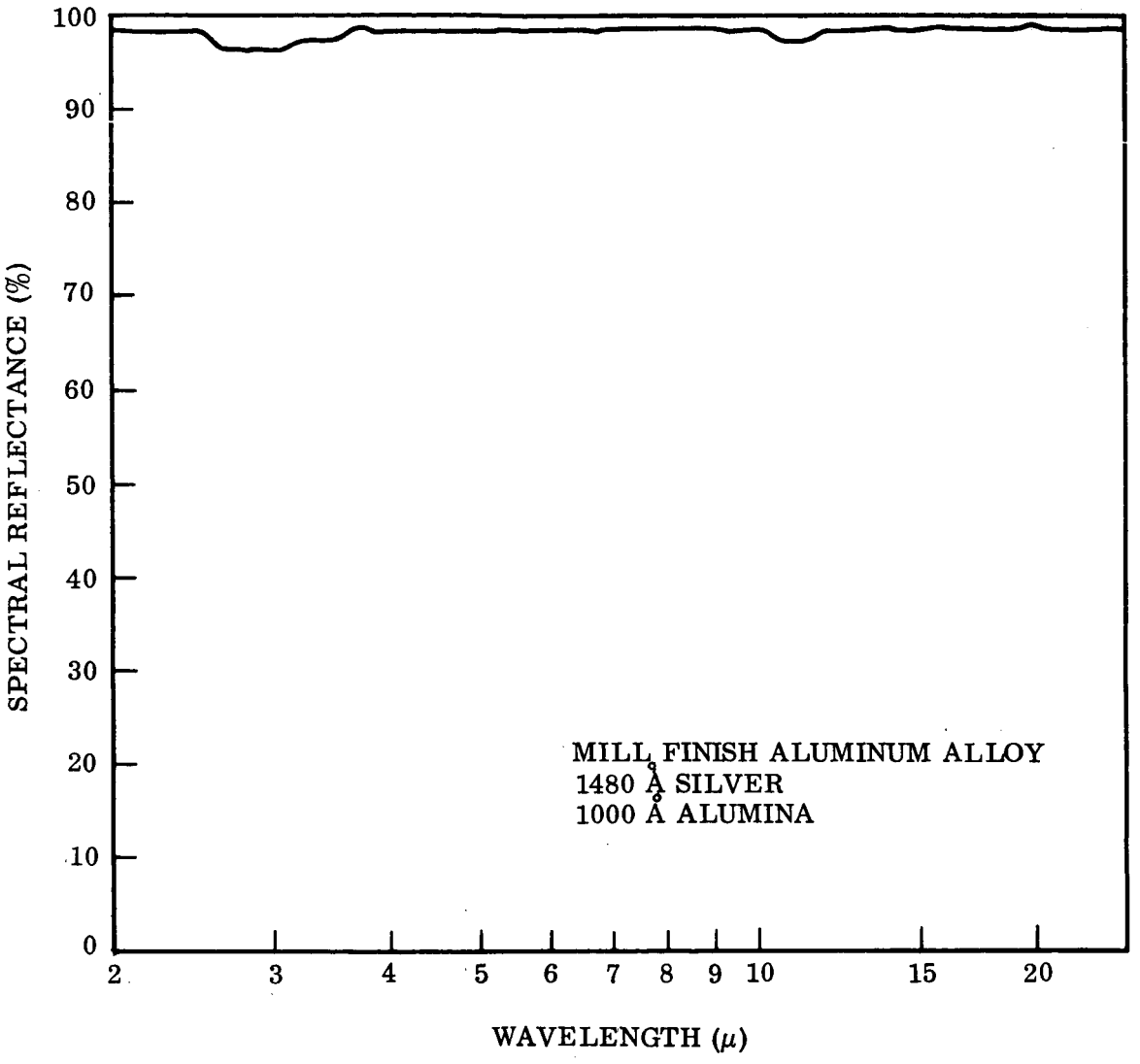

Fig. 7-2 Spectral Reflectance of Alumina-Silver-Aluminum Alloy System

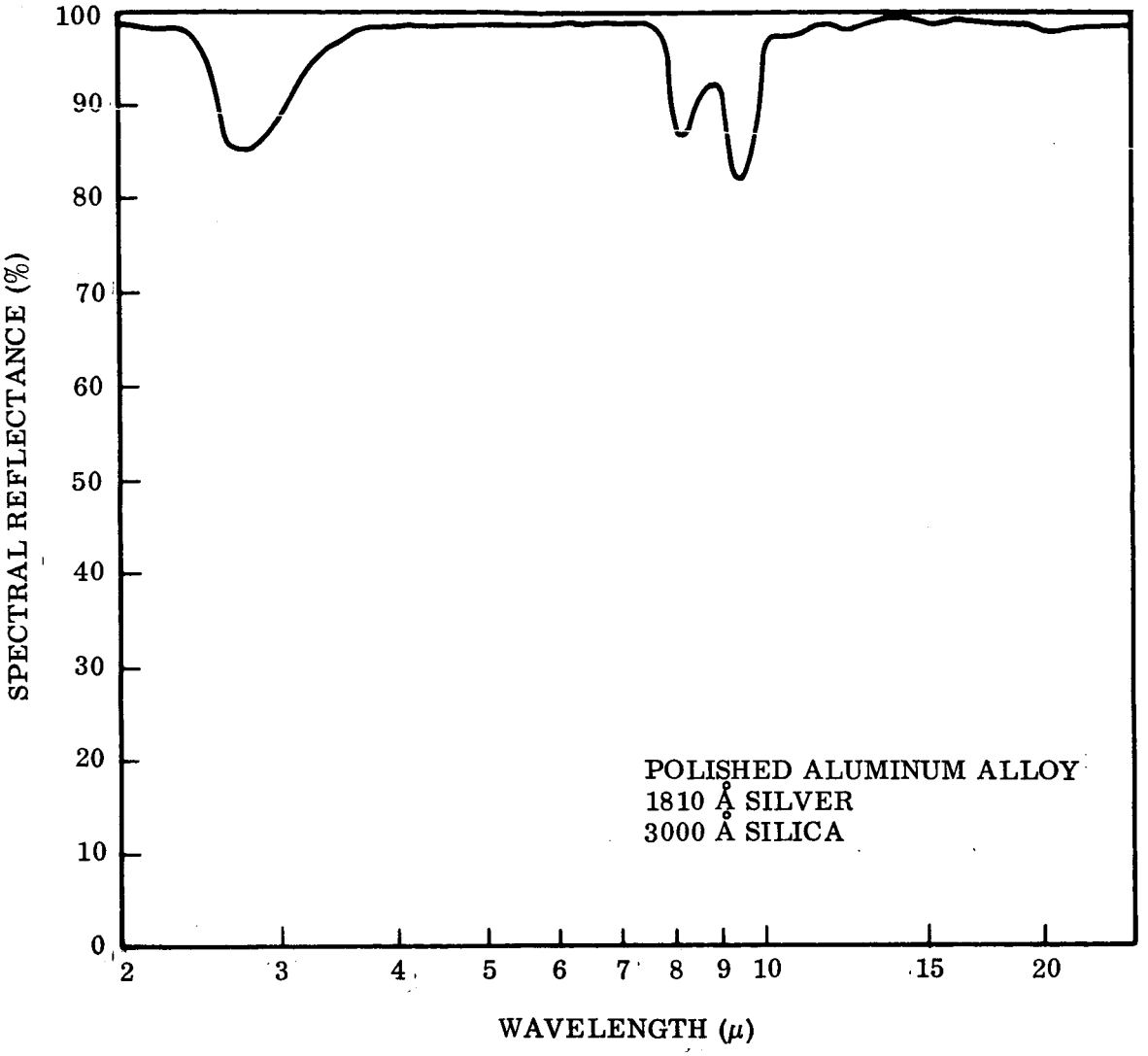

Fig. 7-3 Spectral Reflectance of Silica-Silver-Aluminum Alloy System

was calculated at a series of temperatures by integrating over the appropriate Planckian distribution. In the case of the Optical Solar Reflector, the normal and hemispherical emittances agreed to within 10% as would be anticipated on the basis of the thickness of the fused silica emitting surface. This thickness of the dielectric ensures that the absorption bands are saturated, so that directional emittance effects are minimized. The measured emittance is characteristic of bulk fused silica and is limited in magnitude by the strong characteristics Restrahlen band near 9 μ. The calculations of normal emittance as a function of temperature indicate a maximum in the vicinity of 400° K, at which temperature the maximum of the corresponding blackbody curve coincides with the minimum reflectance of this system.

In contrast to the OSR, the alumina-silver-aluminum alloy system shows virtually no spectral structure in the 2- to 25-μ region, and the calculated normal reflectance is essentially invariant over the temperature range 294−555° K. Owing to the thin (1000 Å), essentially transparent overlay of alumina, the normal emittance is nominally that of the opaque silver film on the substrate. However, at angles far from the normal, the effective thickness of dielectric which is traversed by emitted photons is significantly greater than the physical dimensions of the dielectric film. Consequently, the effective absorptance (and emittance) is increased, as reflected in the measured value of total hemispherical emittance. At 300° K, the ratio of ϵ_H/ϵ_N is greater than 3, in agreement with the work of Hass et al. (Ref. 6) on similar systems.

The system silica-silver-aluminum alloy presents an intermediate case, in which well-defined but weak absorption bands occur in the infrared region. As a result, the normal emittance is greater than the alumina-silver system and exhibits a more pronounced temperature dependence. In this case, as well, ϵ_H is significantly greater than ϵ_N, in accordance with the calculations of Hass et al. for the analogous case of SiO films.

The relationships between normal emittance and total hemispherical emittance are poorly defined for the systems studied in the course of this program. The conventional

method of calculating ϵ_H from spectrally generated normal emittance based on the use of Jacob's relationships (Ref. 16) is not applicable to coatings that are partially transparent. On this basis, accurate determination of emittance for systems of this type is limited to calorimetric techniques, which are tedious and time consuming.

The alternate techniques (Lion Optical Surface Comparator and spectral reflectance) are valuable, however, for determining changes in emittance of the coating systems as a result of environmental exposures or variation of the coating process parameters.

Section 8
CONCLUSIONS

The results of this program conclusively demonstrate the feasibility of employing vacuum-deposited coatings for thermal control applications on Mars entry capsules and for near-solar missions. The practicality of tailoring the optical properties of metal-dielectric films by appropriate choice of materials and deposition parameters has been established.

The initial goals set forth at the inception of the program have been achieved. The requirements for systems with the three sets of properties (1) $\alpha_s/\epsilon < 0.1$, (2) $\alpha_s/\epsilon \approx 1$ with $\alpha_s < 0.1$, and (3) minimum emittance,have been met by the Optical Solar Reflector (a second surface mirror employing silvered fused silica), the silica-silver-aluminum alloy system, and the alumina-silver-aluminum alloy system, respectively.

The minimum emittance system (alumina-silver-aluminum alloy) has low normal emittance (0.014) but a much higher hemispherical emittance (0.057).

In addition, the feasibility of applying OSR to curved surfaces in the form of structural members with large L/D ratios has been demonstrated.

The environmental stability of the OSR system has been shown to be exceptionally promising, with little or no change in the optical properties noted for extended ultraviolet irradiation and thermal cycling between 294°K and 533°K. This type of stability is a prerequisite for candidate thermal control coating systems for near-solar missions where elevated equilibrium temperature conditions prevail, as well as for extended missions of increased sophistication requiring more predictable thermal control properties than afforded by conventional painted coating.

The silica-silver-aluminum alloy system and the alumina-silver-aluminum alloy system exposed to UV irradiation at 294°K showed minor degradation in solar absorptance. The alumina-silver-aluminum alloy system showed large degradation at 533°K. This is ascribed to thermal diffusion of the coating into the substrate which may be controlled by use of diffusion barriers.

The objectives of this program did not include a study of the mechanical properties of the dielectric overcoating materials. However, from observations made during the processing of these dielectric films, they appear to have excellent abrasion resistance and can be handled and cleaned with a minimum of precautions. The aluminum oxide is stable at room temperature and is preferable because of better thermal expansion matching to metal surfaces.

The Optical Solar Reflector, although possessing the most favorable characteristics for near-solar mission thermal control (low α_s/ϵ), must be bonded to the substrate via adhesive or mechanical fasteners. However, because of its low weight per unit area (0.056 gm/cm^2), it can be used on a competitive basis with conventional thermal control paints.

The electron beam evaporated coatings, on the other hand, being applied directly to the substrate, lead to three orders of magnitude advantage in weight savings by virtue of their thin-film configuration. However, maximum emittance attainable with these coatings is 80 percent of the OSR system.

The OSR coating system investigated in the course of this program can be considered to constitute a second generation of thermal control coatings that exhibits exceptional optical thermal and environmental properties. The dielectric overcoated metal systems offer the advantages of flexibility in the variation of emittance by controlling the thickness of the dielectric overlay. This approach to thermal control of space vehicles offers considerable promise from the standpoint of meeting the system requirements dictated by the increasing sophistication and environmental demands of future long-duration earth orbital and interplanetary space missions.

Section 9
RECOMMENDATIONS

On the basis of the results of this program, several areas requiring further examination in depth are indicated. Only through a more detailed understanding of the physical and optical properties of these systems can this approach be reduced to practical engineering procedures.

The specific areas requiring further studies include:

- Investigation of greater thicknesses of dielectric in order to approach bulk emittance properties
- Investigation of dielectric-diffusion barriers between the substrate and metallic films
- Investigation of environmental parameters such as long-term thermal exposure, ultraviolet, and particulate radiation (electrons and protons), separately and in combination, in order to evaluate possible synergistic effects
- Investigation of approaches to extend these systems to higher temperature ranges in accordance with 0.05 AU projected missions
- Metallographic examination of film morphology and metal-dielectric interactions
- Investigation of the concept of mixed oxide dielectric overlays for maximizing emittance via Restrahlen repression

Any anticipated continuation of efforts related to this program should be based on sound scientific reasoning rather than engineering requirement exclusively, in order to attain a coherent understanding of the properties and performance of realistic systems.

Section 10
REFERENCES

1. Optical Solar Reflector (LMSC 3-56-65-2), Thermal Control Surface, Contract AF 04(647)-787
2. R. P. Caven, Chapter I, Thermal Radiation Properties of Solids, Progress in Astronautics and Aeronautics, Vol. 18, edited by G. B. Heller, Academic Press, New York, 1966, pp. 61
3. C. F. Powell, J. H. Oxley, and J. M. Blocher, Vapor Deposition, Wiley, New York, 1966
4. G. Hass, ed., Physics of Thin Films, Vol. I, Academic Press, New York, 1963
5. G. Hass and R. E. Thun, Physics of Thin Films, Vol. II, Academic Press, New York, 1964
6. G. Hass, J. B. Ramsey, J. J. Triolo, and H. T. Albright, AIAA Paper No. 65-656, Thermophysics Specialist Conference, Monterey, Calif., 13–15 Sep 1965
7. G. A. Bassett, J. W. Menter, and D. W. Pashley, "The Nucleation, Growth, and Microstructure of Thin Films," Structures and Properties of Thin Films, ed. by Neugebauer, Newkirk, Vermilyea, Wiley, New York, 1959
8. E. M. Van Vliet, Passive Temperature Control in the Space Environment Macmillan, New York, 1965
9. L. Holland, Thin Film Microelectronics, Wiley, New York, 1965
10. L. Holland, Vacuum Deposition of Thin Films, Wiley, New York, 1956
11. C. A. Neugebauer, "The Structure and Properties of Thin Films," Transactions of the Third International Vacuum Congress, Vol. 1, Pergamon, London, 1966
12. L. Addicks, Silver in Industry, Reinhold, New York, 1940

13. T. L. Rollins, F. L. Weichman, Physica Status Solidi, 15, 233 (1966)

14. R. L. Fullman, "Boundary Migration During Grain Growth," Metal Interfaces, ASM, 1952

15. P. A. Beck, "Interface Migration in Recrystallization," Metal Interfaces, ASM, 1952

16. M. Jacob, Heat Transfer, Vol. 2, Wiley, New York, 1949